

VERTEX 2014

23rd International Workshop on Vertex Detectors

Mácha Lake | Doksy, Czech Republic



September 15 - 19, 2014

RD50 overview

RD50: Radiation hard semiconductor devices for high luminosity colliders

Marcos Fernandez Garcia^{1,2}
on behalf of the RD50 collaboration



¹Instituto de Física de Cantabria, IFCA-Santander, Spain

²Visiting scientist at CERN-PH-DT SSD lab

Outline

Past: The findings of the ROSE collaboration

Present: The RD50 collaboration
From microscopic defects to macroscopic properties
Simulating device performance
Choice of Materials for HL-LHC
Charge multiplication after heavy irradiation
From future to present: 3D sensors

Near present:
New devices: HVCMOS

Some history: the ROSE collaboration

RD48 (ROSE collaboration): 1996-2001

ROSE collaboration: 38 groups, 7 associated companies, 3 observers by 2001

Main outcomes:

- **Oxygen enrichment of Si bulk** → Radiation hardening against charged hadrons → Choice of DOFZ material for pixel sensors (fluence dominated by charged hadrons)

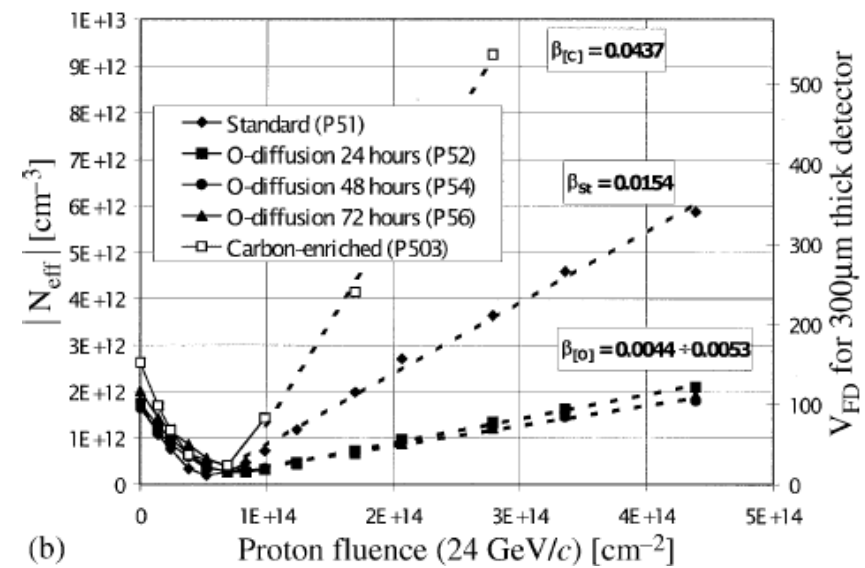
Method: Diffusion of oxygen from a thick oxide layer grown via a prolonged oxidation step

Microscopical reason at that time not clear

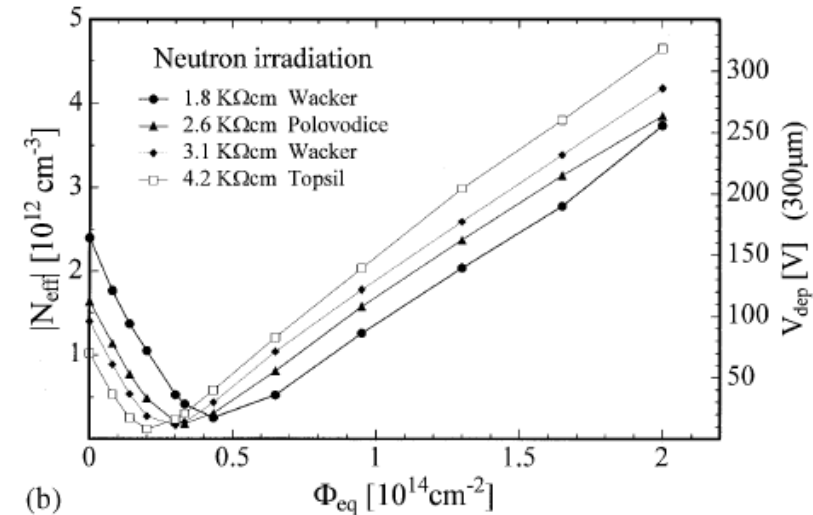
- **“Low” resistivity Si (1 kΩ.cm) beneficial** for delayed type inversion after **neutron** irradiation

- **Hamburg model** (prediction of type inversion point and long term behavior of the effective doping concentration N_{eff}) → **projection** of damage results to LHC operational conditions

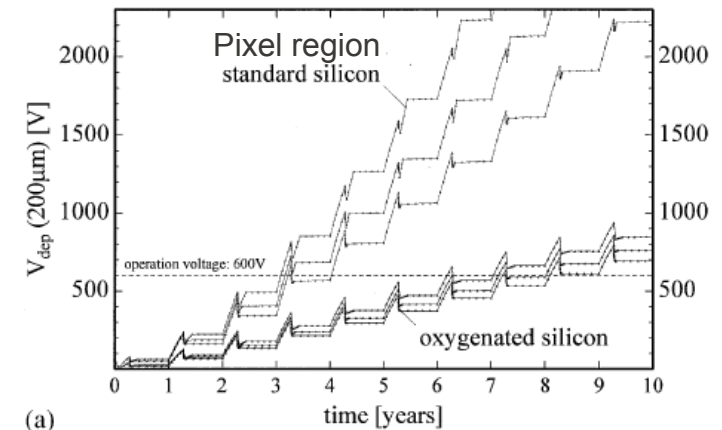
Plots from G. Lindstrom et al, NIMA 466 (2001) 308-326



(b)



(b)



(a)

Present times: the RD50 collaboration

The RD50 collaboration

From microscopic defects to macroscopic properties

Simulating device performance

Choice of Materials for HL-LHC

Charge multiplication after heavy irradiation

From future to present: 3D sensors

The RD50 Collaboration

- **RD50: 50 institutes and 275 members**

42 European and Asian institutes

Belarus (Minsk), Belgium (Louvain), Czech Republic (Prague (3x)), Finland (Helsinki, Lappeenranta), France (Paris, Orsay), Greece (Demokritos), Germany (Dortmund, Erfurt, Freiburg, Hamburg (2x), Karlsruhe, Munich(2x)), Italy (Bari, Florence, Perugia, Pisa, Torino), Lithuania (Vilnius), Netherlands (NIKHEF), Poland (Krakow, Warsaw(2x)), Romania (Bucharest (2x)), Russia (Moscow, St.Petersburg), Slovenia (Ljubljana), Spain (Barcelona(2x), Santander, Valencia), Switzerland (CERN, PSI), Ukraine (Kiev), United Kingdom (Glasgow, Liverpool)



6 North-American institutes

Canada (Montreal), USA (BNL, Fermilab, New Mexico, Santa Cruz, Syracuse)

1 Middle East institute

Israel (Tel Aviv)

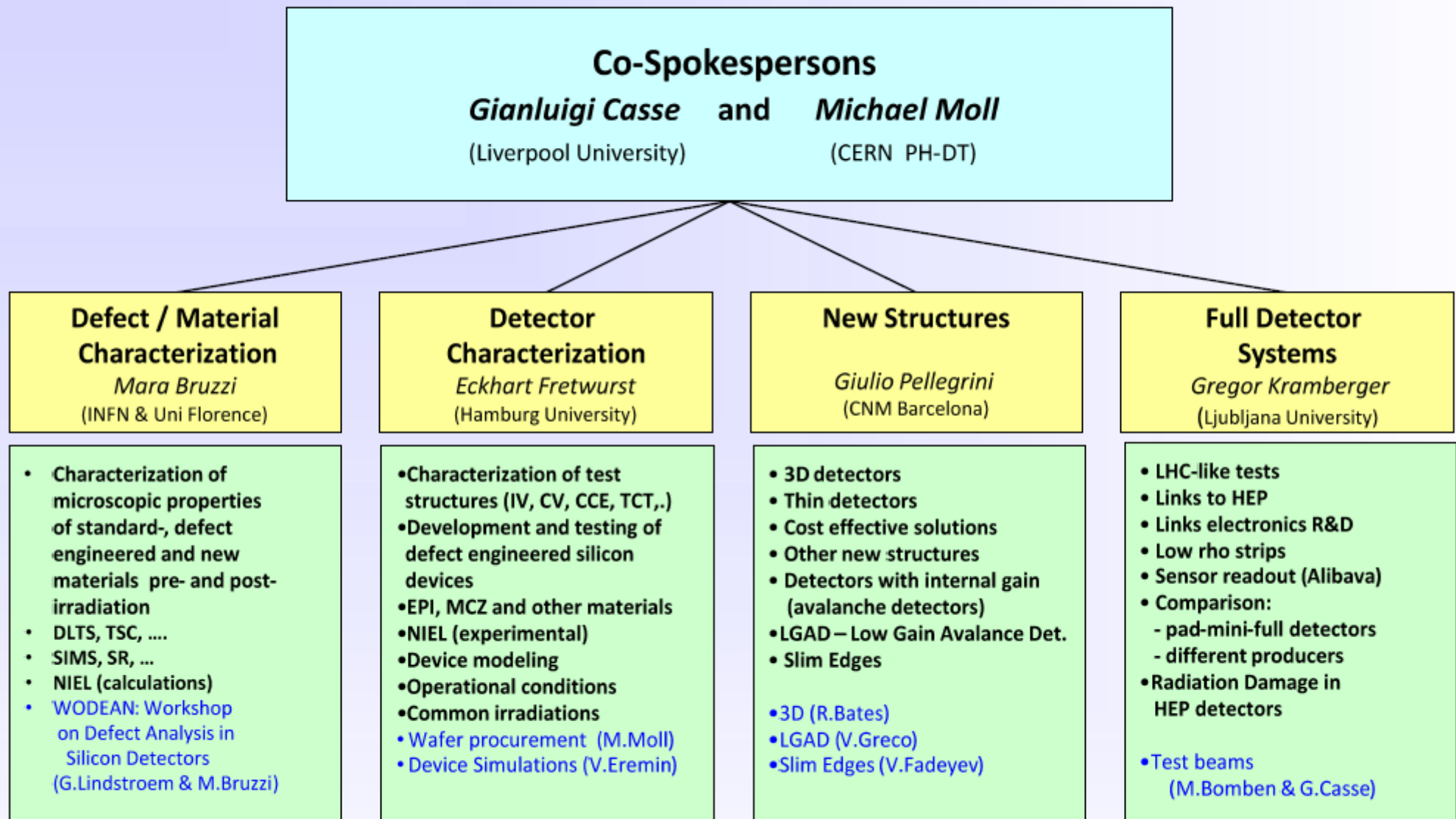
1 Asian institute

India (Delhi)

Detailed member list: <http://cern.ch/rd50>

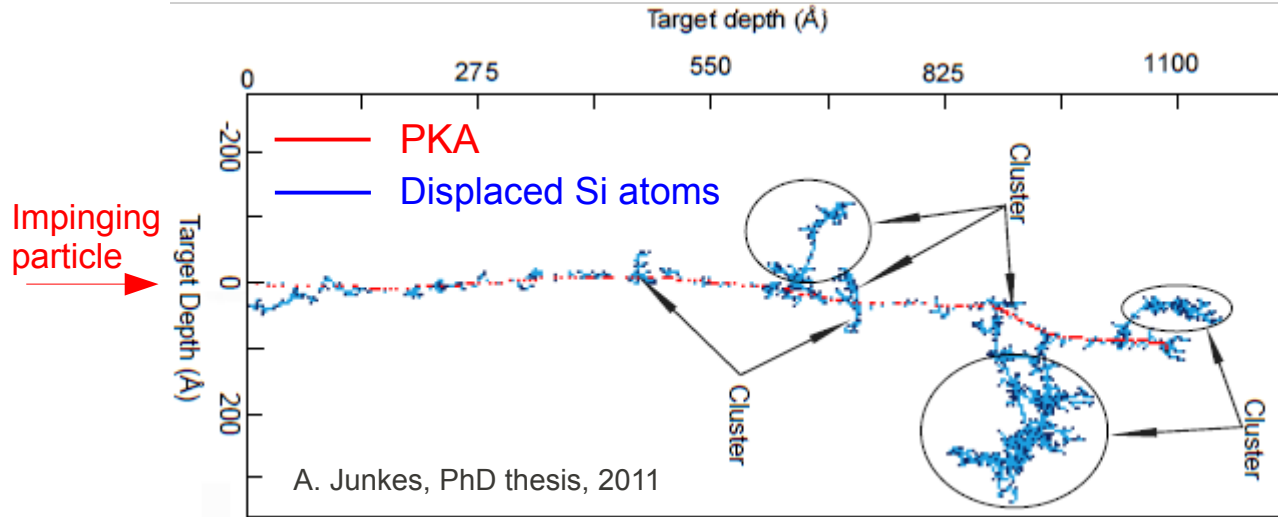
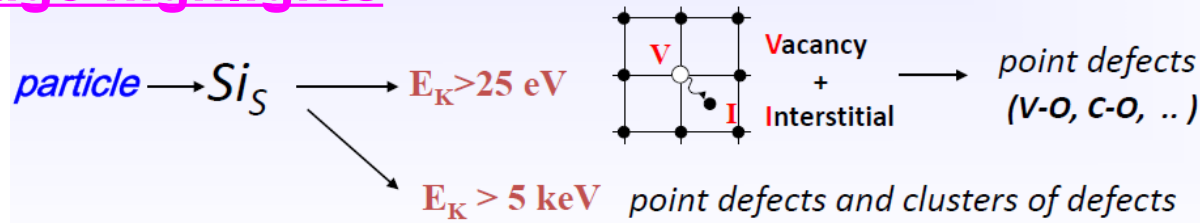


RD50 Organizational Structure



Collaboration Board Chair & Deputy: G.Kramberger (Ljubljana) & J.Vaitkus (Vilnius), Conference committee: U.Parzefall (Freiburg)
CERN contact: M.Moll (PH-DT), Secretary: V.Wedlake (PH-DT), Budget holder & GLIMOS: M.Glaser (PH-DT)

Radiation damage highlights



Simulation of the damage created by a knocked on Si atom with recoil energy of 50 keV (~average kinetic energy transferred by a 1 MeV neutron to a PKA)

^{60}Co -gammas

- Compton Electrons with max. $E_\gamma \approx 1 \text{ MeV}$ (no cluster production)

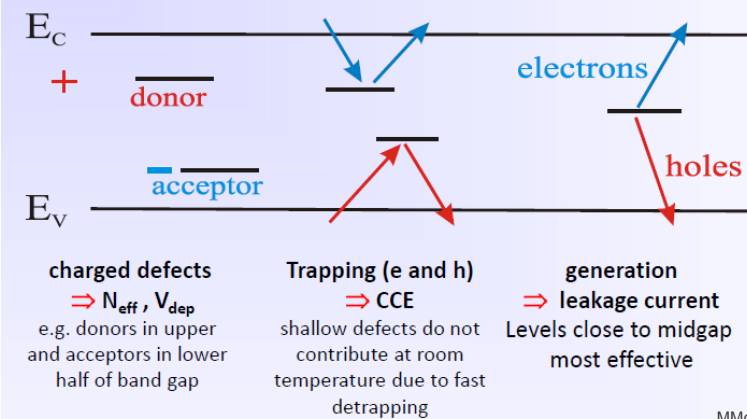
Electrons

- $E_e > 255 \text{ keV}$ for displacement
- $E_e > 8 \text{ MeV}$ for cluster

Neutrons (elastic scattering)

- $E_n > 185 \text{ eV}$ for displacement
- $E_n > 35 \text{ keV}$ for cluster

Only point defects \leftrightarrow point defects & clusters \leftrightarrow Mainly clusters



$N_{\text{eff}} \uparrow$

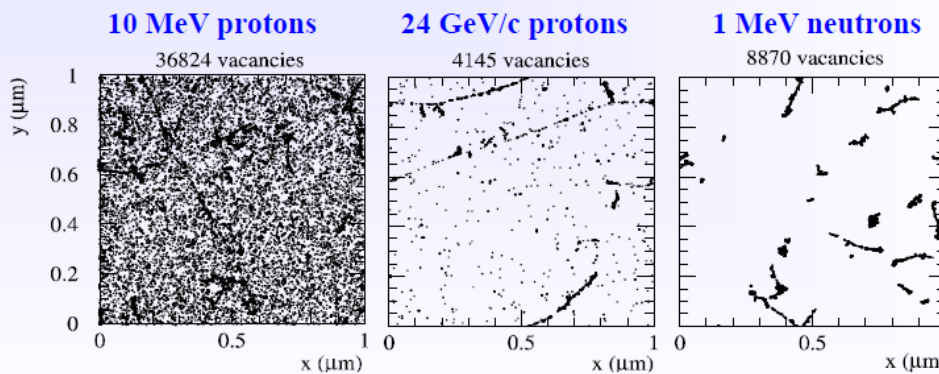
$CC(\downarrow)$

$I_{\text{leak}} \uparrow$

Simulation:

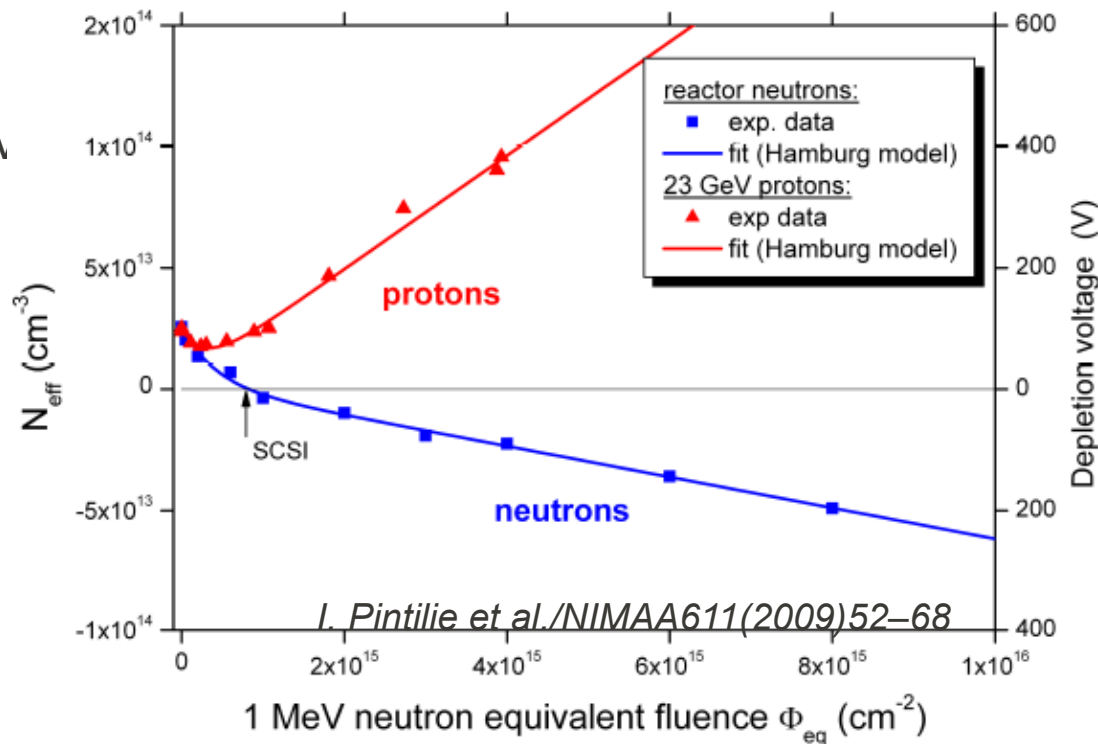
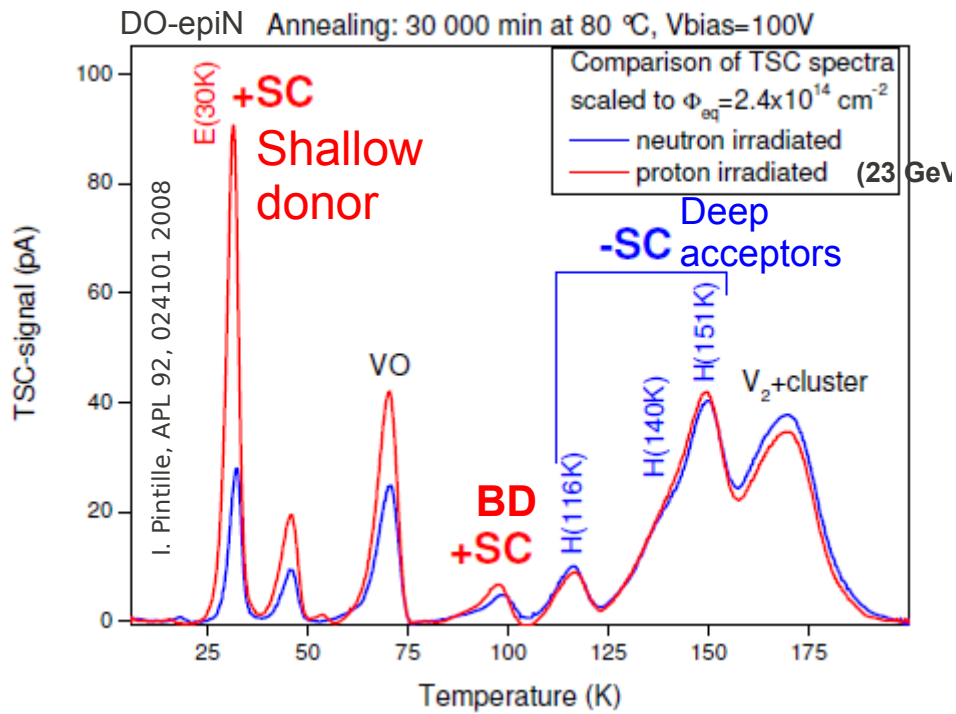
Initial distribution of vacancies in $(1\mu\text{m})^3$ after 10^{14} particles/cm²

[Mika Huhtinen NIMA 491(2002) 194]



Defects with impact on Neff

- Significant progress over last few years identifying defects responsible for sensor degradation after neutron and proton irradiation. Defects related to N_{eff} and reverse annealing



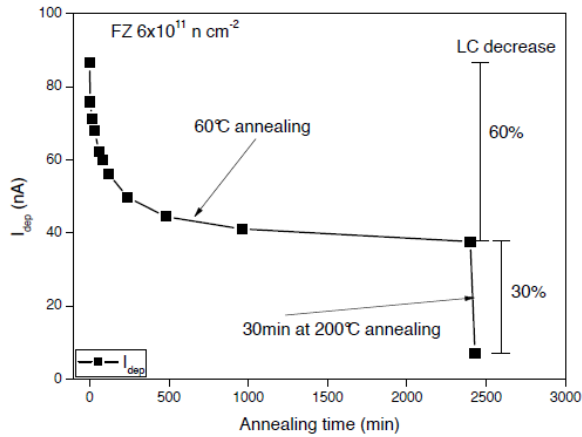
– Identified **shallow donors [E(30K) and BD]** in O-rich epi-Si with higher concentration after proton than after neutron irradiation. They contribute with +sc (positive space charge). VP process also suppressed.

The peaks for deep acceptors (identified as hole traps, **H(116K),H(140K),H(152K)**) responsible for reverse annealing. Observed concentration increase with time at 80 C.

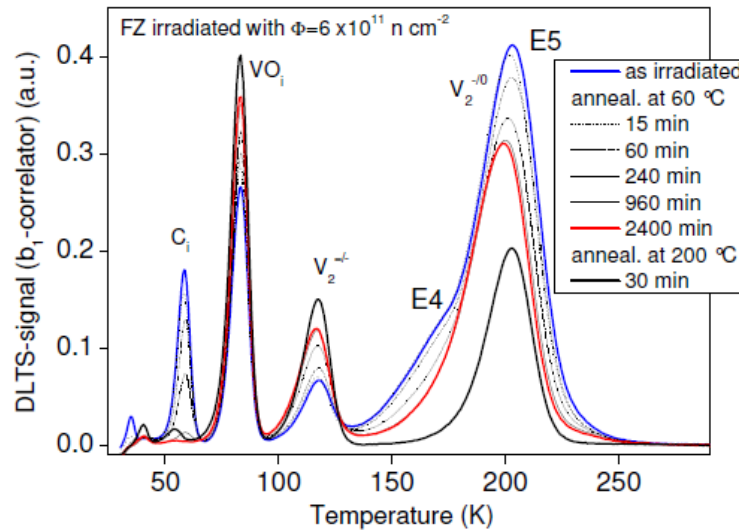
The concentration of **positive space charge** overcomes that of **deep acceptor (-sc)**. As a consequence no type inversion after proton irradiation seen in O-rich materials.

[overcompensation of +sc for short annealing times in DO-Epi material]

Defects with impact on leakage current



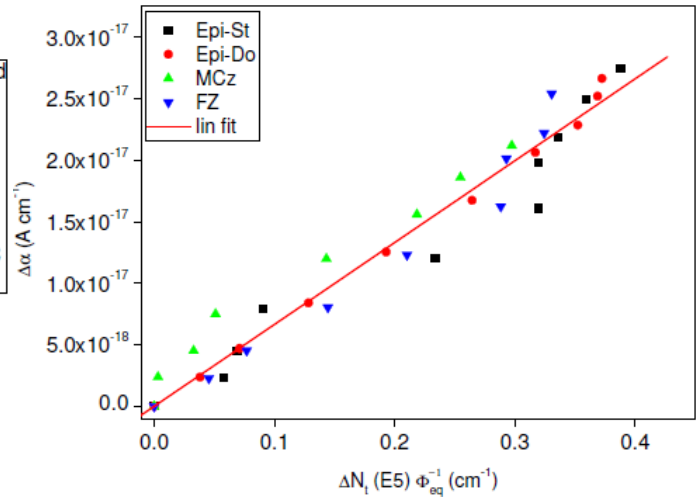
Leakage current annealing with time at 60C



DLTS peaks proportional to defect concentration.

Defects with impact on leakage current have to be near the middle of the band gap.

Peak at 200K consists of several defects and “dissolves” with time and temperature. It correlates with the annealed fraction of leakage current.



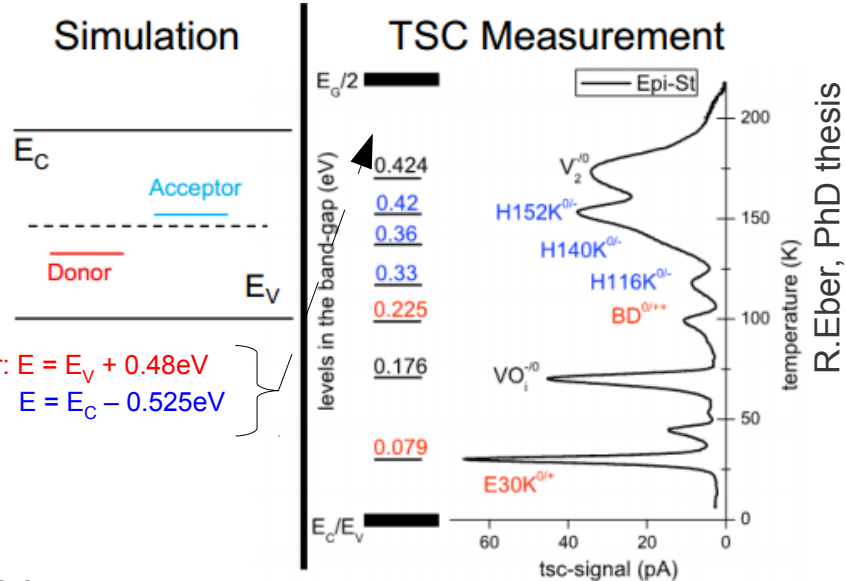
Correlation of the E5 concentration with the change of damage parameter α in Si

Trapping: Indications that E205a (leakage) and H152K (N_{eff}) are important (further work needed)

Defects implementation into simulations

Measured defects not used in TCAD programs. Instead replaced by few (2-5) “effective” levels that reproduce measurements (I_{leak} , V_{dep} , TCT and CCE). Also different sets for proton and neutron irradiation

Simulations do **not** make use of **Hamburg model**. Filling of traps by current determines space charge → electric field.



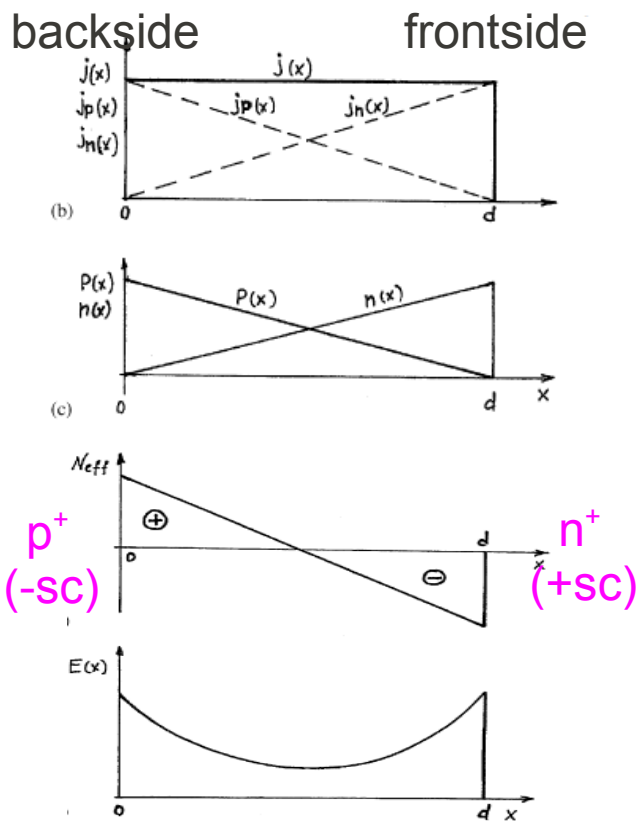
Double Junction:

Type inversion is a simplification of real process. Two junctions appear after traps are filled.

There can be a resistive, non depleted region in between the junctions.

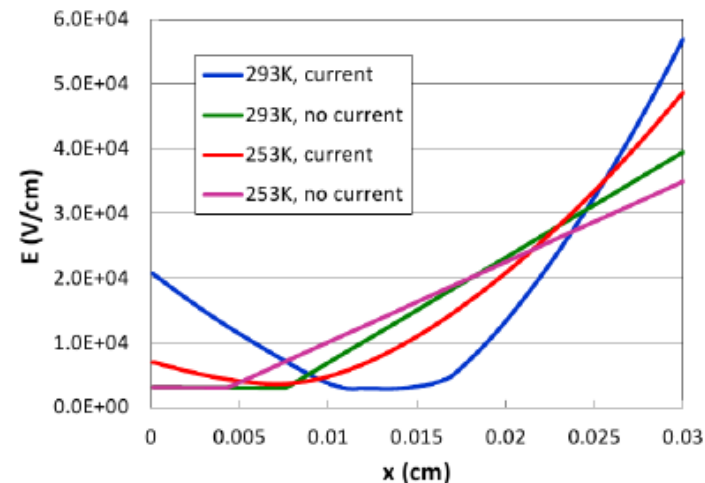
Under reverse bias → voltage drop across it, leads to an electric field, even if it is not depleted!!

Neff as **single parameter** describing the inversion is inaccurate.



V. Eremin, A 476 (2002) 556–564

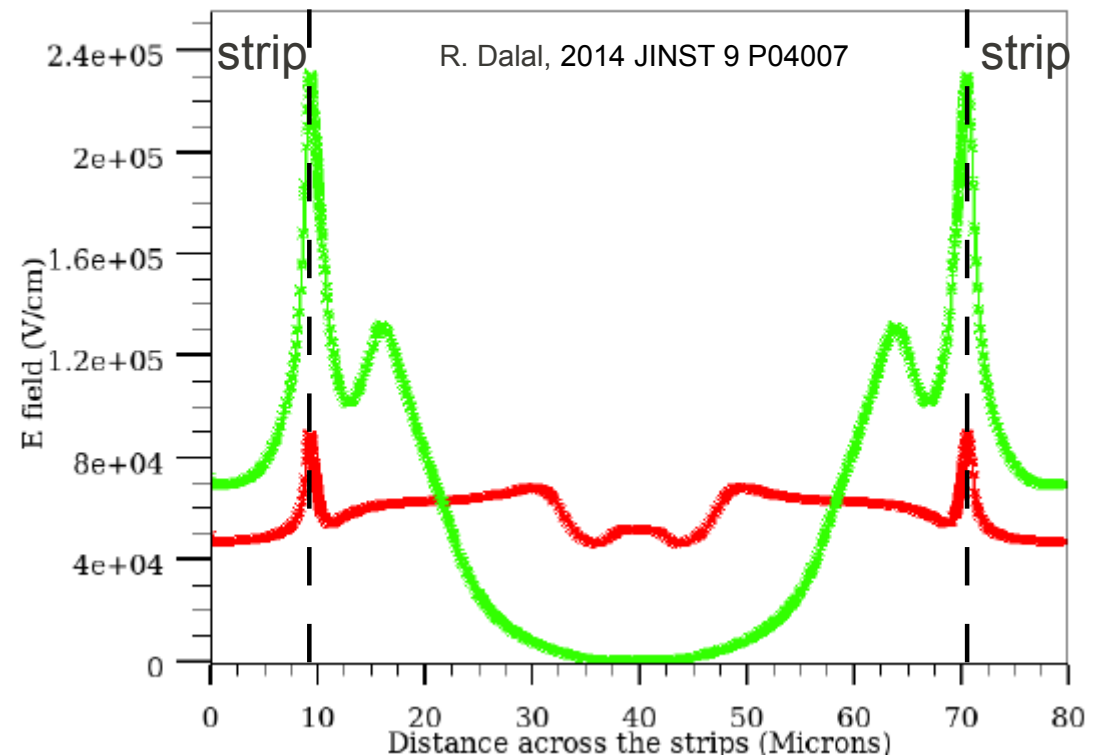
E. Verbitskaya, 21st RD50 Workshop



Bulk and surface damage

- Despite the fact that our community has always concentrated in the **bulk damage** of detectors, both *bulk and surface damage* take place simultaneously
- The **design** of the detectors has to be **adjusted** in a way that the changes in the electric field due to the **oxide charges** *do not influence the sensor performance*
- Bulk and Surface damage are included into TCAD simulations by RD50. For surface damage both **oxide charge density and Interface traps** are being implemented. [\[Details in Ranjeet's talk tomorrow\]](#).

E field for p-on-n and n-on-p type strip sensors for Fluence= $1e15cm^{-2}$
Qf= $1.2e12cm^{-2}$, Bias=500V, Cutline is 1.4um below SiO₂/Si



- Some effects can only be simulated taking into account surface damage effects. Right: comparison of electric fields of **n-on-p** and **p-on-n** type strip sensors after proton fluence of 10^{15} neq/cm², considering oxide charge densities 1.2×10^{12} cm⁻².
- Higher E-field in p-on-n sensor at the strip can produce microdischarges and lead to so-called Random Ghost Hits.

Simulation matching with measurements (effective 2 trap model)

Proton model

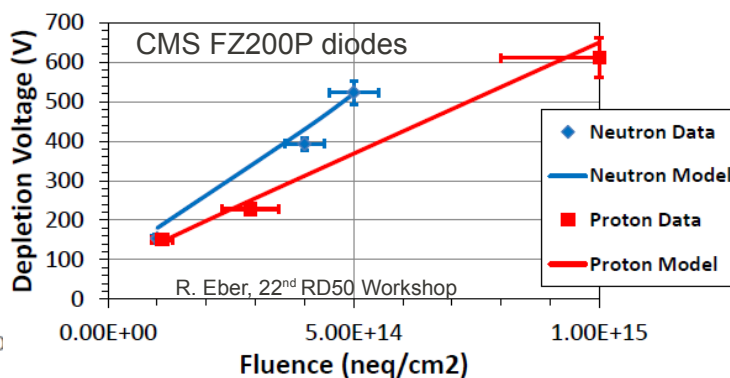
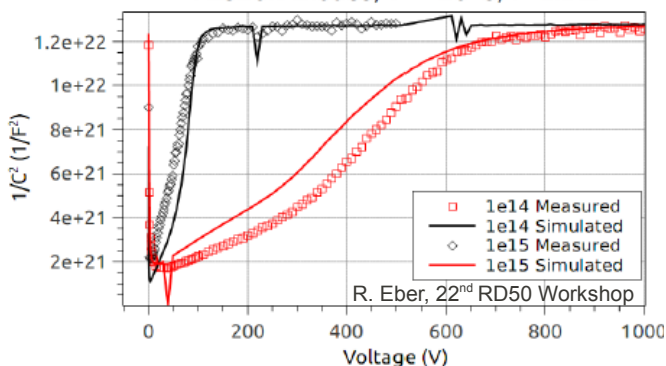
Type of defect	Level [eV]	σ_e [cm ²]	σ_h [cm ²]	Concentration [cm ⁻³]
Deep acceptor	$E_C - 0.525$	$1e-14$	$1e-14$	$1.189 \cdot F + 6.454e13$
Deep donor	$E_V + 0.48$	$1e-14$	$1e-14$	$5.598 \cdot F - 3.959e14$

Neutron model

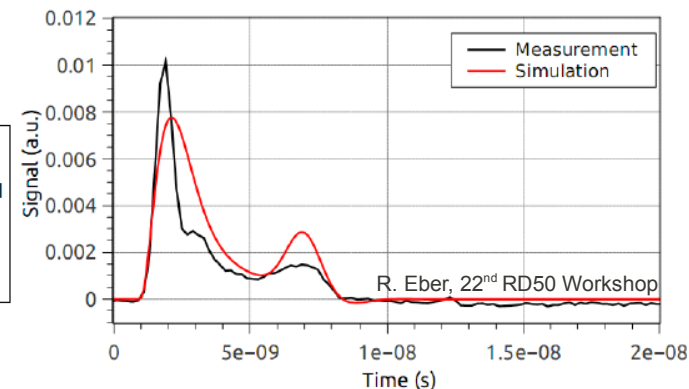
Type of defect	Level [eV]	σ_e [cm ²]	σ_h [cm ²]	Concentration [cm ⁻³]
Deep acceptor	$E_C - 0.525$	$1.2e-14$	$1.2e-14$	$1.55 \cdot F$
Deep donor	$E_V + 0.48$	$1.2e-14$	$1.2e-14$	$1.395 \cdot F$

$$\Phi = [10^{14} - 10^{15}] n_{eq} / \text{cm}^2$$

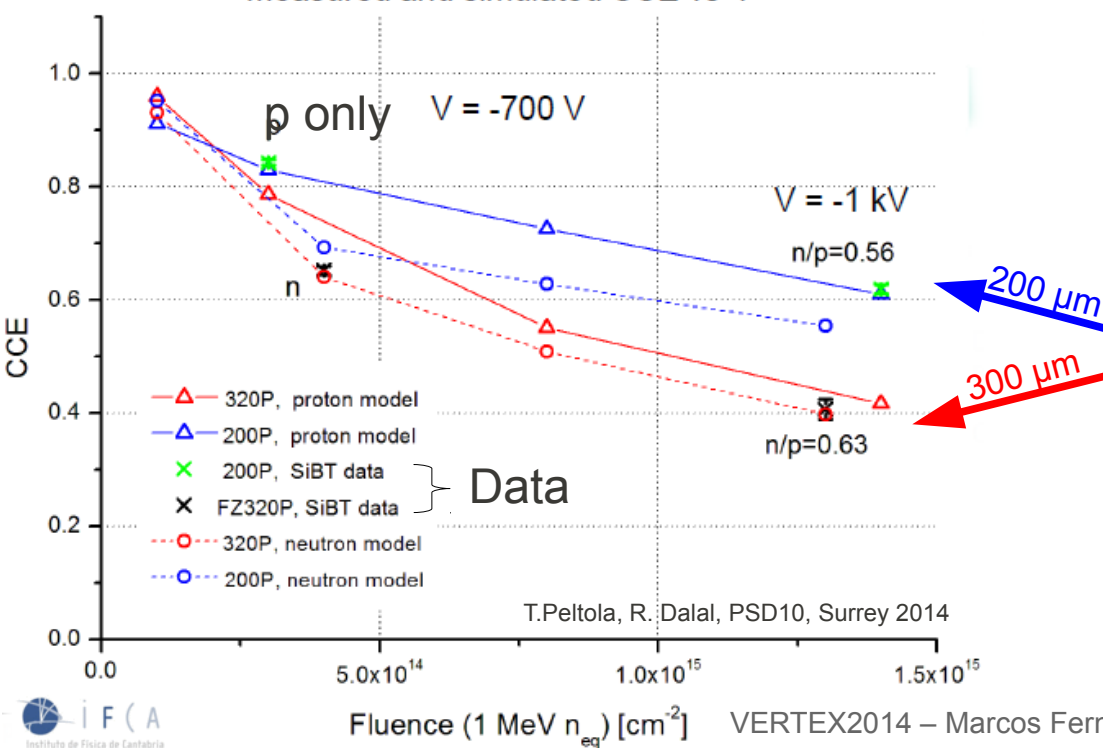
Comparison of Simulated and Measured CV
FZ320N Diodes, T = -20°C, f = 1kHz



TCT Signal
F = 1e15 neq/cm², T = -20°C, V = 400V



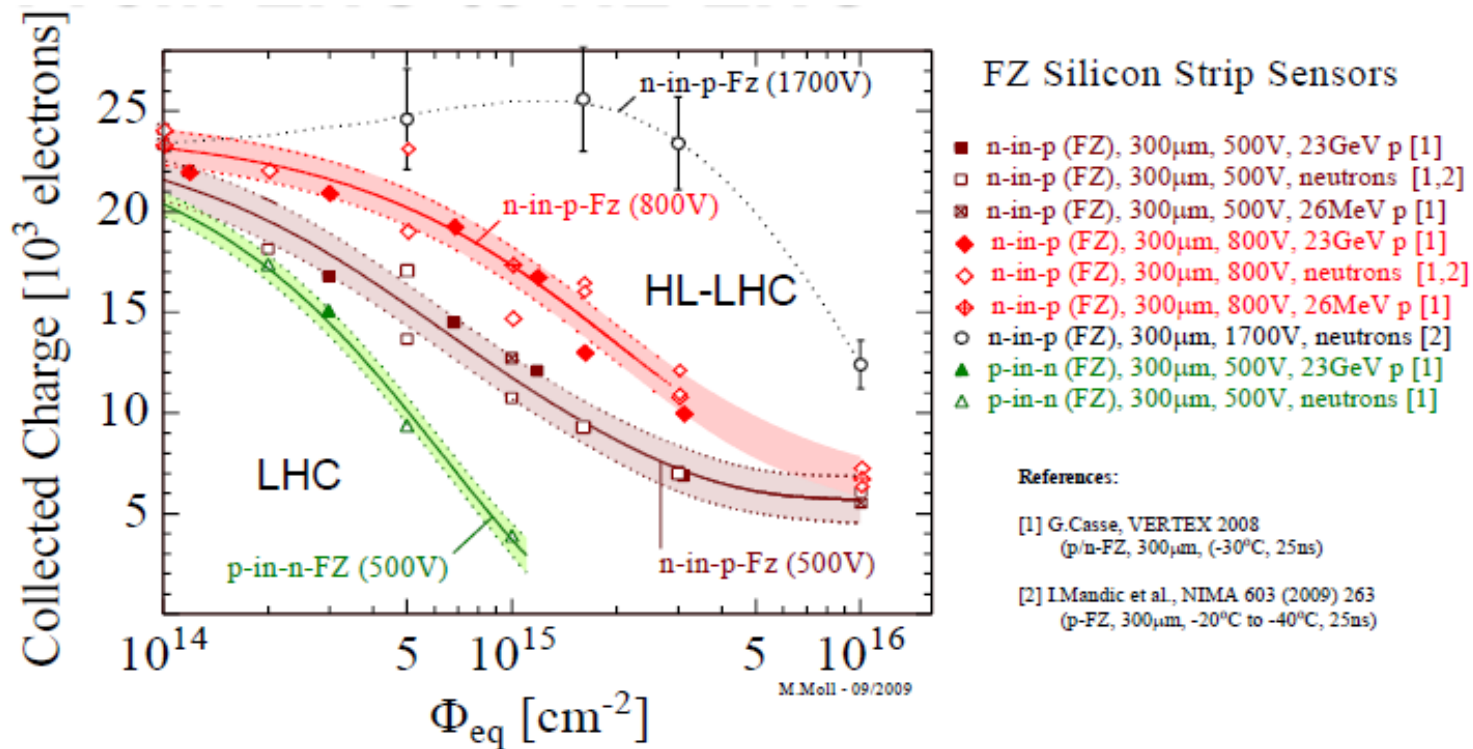
Measured and simulated CCE vs Φ



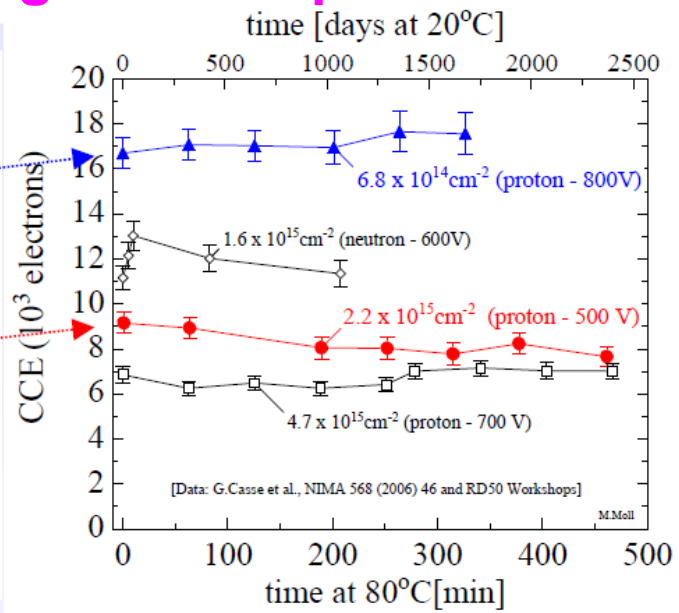
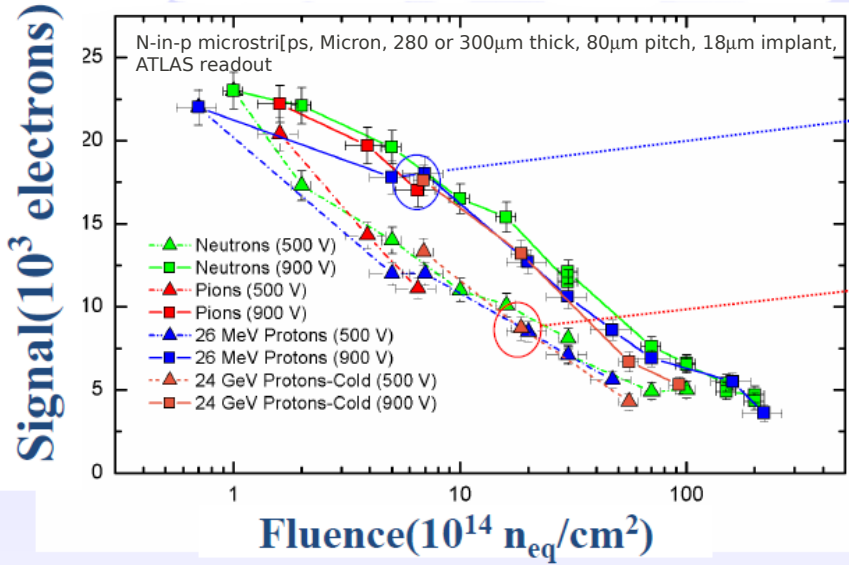
- CCE simulations using 2 trap model + fixed charges at Si/SiO₂ interface
- Model predicts test beam measured CCE (trapping!) of FZ320P and MCZ+FZ200P samples proton irradiated, neutron and mixed!
- Leakage current predicted correctly

Choice of Silicon material for HL-LHC

- P-type silicon brought forward by RD50. Now baseline for CMS and ATLAS tracker upgrades
- Reasons for this choice:
 - Electric field and weighting field are maxima at the same electrode ($\vec{E} \cdot \vec{E}_w$ maximum)
 - Electron collection superior over hole collection:
 - 1) **Faster mobility** for electrons
 - 2) Electrons can **multiply** at n+ implant
 - 3) Slightly lower **trapping** for electrons than for holes
 - 4) Decrease of trapping prob with **annealing** for electrons

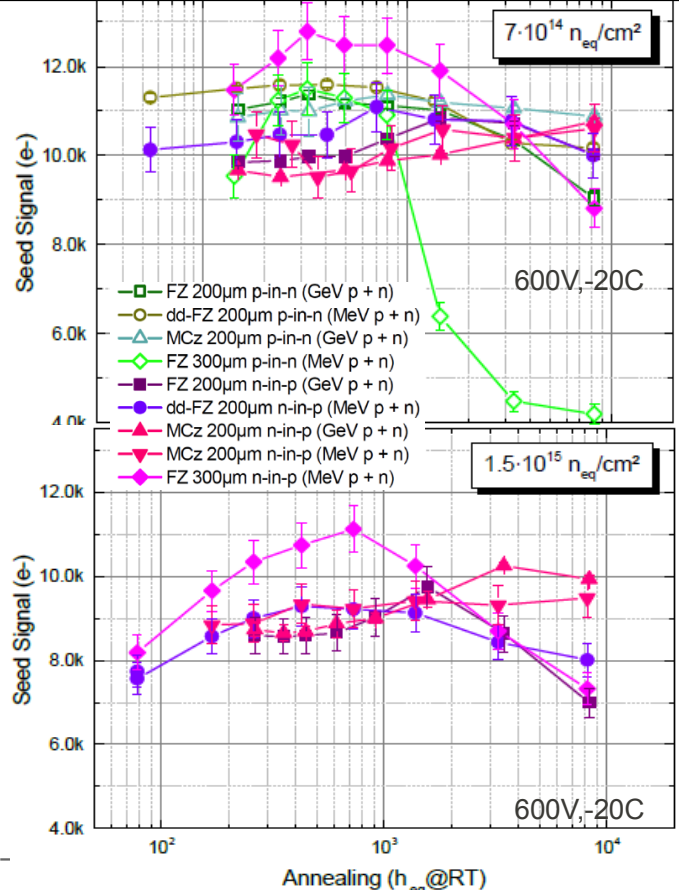
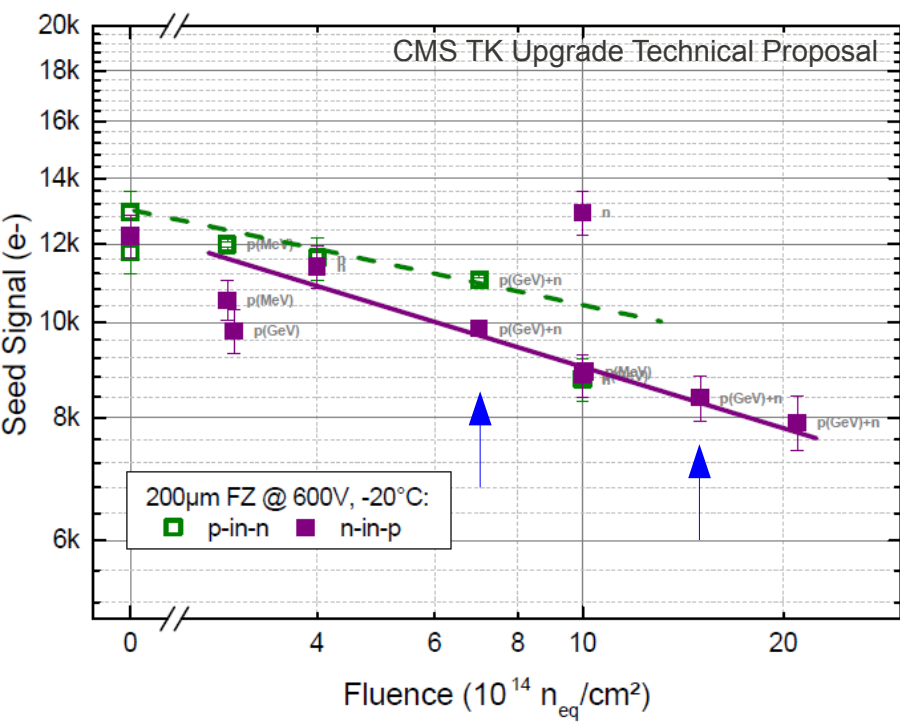


Charge Collection and annealing for n-on-p detectors



ATLAS:

No reverse annealing in CCE measurements for neutron and proton irradiated detectors



CMS:

Left: 200μm n-in-p type sensors show 8ke- seed signal after 2x10¹⁵ neq/cm²

p-in-n type comparable signal but showed increased non-reducible noise and fake hits above

Right: Thicker sensors give more signal but degrade faster.

CC of thin sensors (600V) do not degrade with annealing.

Observation: Charge Multiplication in heavily irradiated detectors

- **Space charge** increase after irradiation ($\Phi \geq 10^{15} \text{ n}_{\text{eq}}/\text{cm}^2$) leads to **high electric field** near the electrodes.
- Charge multiplication (CM) can occur for E-fields $\sim 10\text{-}15 \text{ V}/\mu\text{m}$.
- Collected charge can **exceed** that of the **non-irradiated** detector.
- Observed in **planar** and also in **3D** detectors, n-on-p (electron collection)
- Small **gains** measured < 10 , reason being competition of CM and trapping [E. Verbitskaya et al., NIMA 730 (2013) 66-72]
- CM also increases the current (shot) noise. Noise and signal can have different multiplication factors. For the SNR to increase the capacitive noise should dominate over the shot noise:

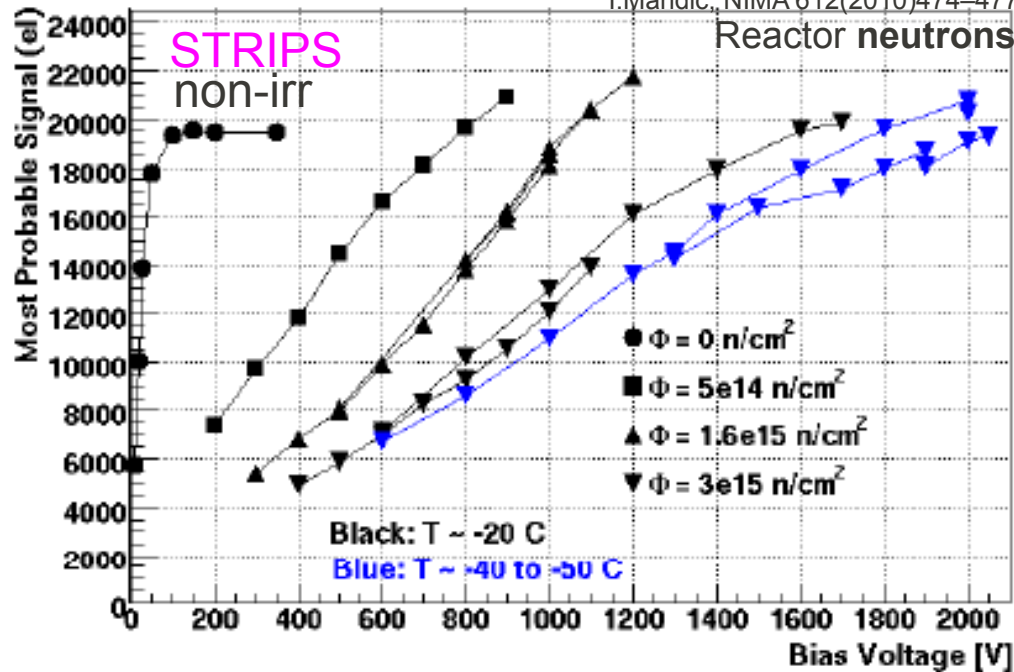
$$SNR = \frac{\bar{Q}}{\sigma_{noise}} = \frac{\bar{Q}}{\sqrt{\sigma_{sh}(M')^2 + \sigma_{noise}'^2}} = \frac{M\bar{Q}_{M=1}}{\sqrt{\sigma_{sh,M'=1}^2 M'^2 F' + \sigma_{noise}'^2}}$$

J. Lange, DESY-THESIS-2013-042

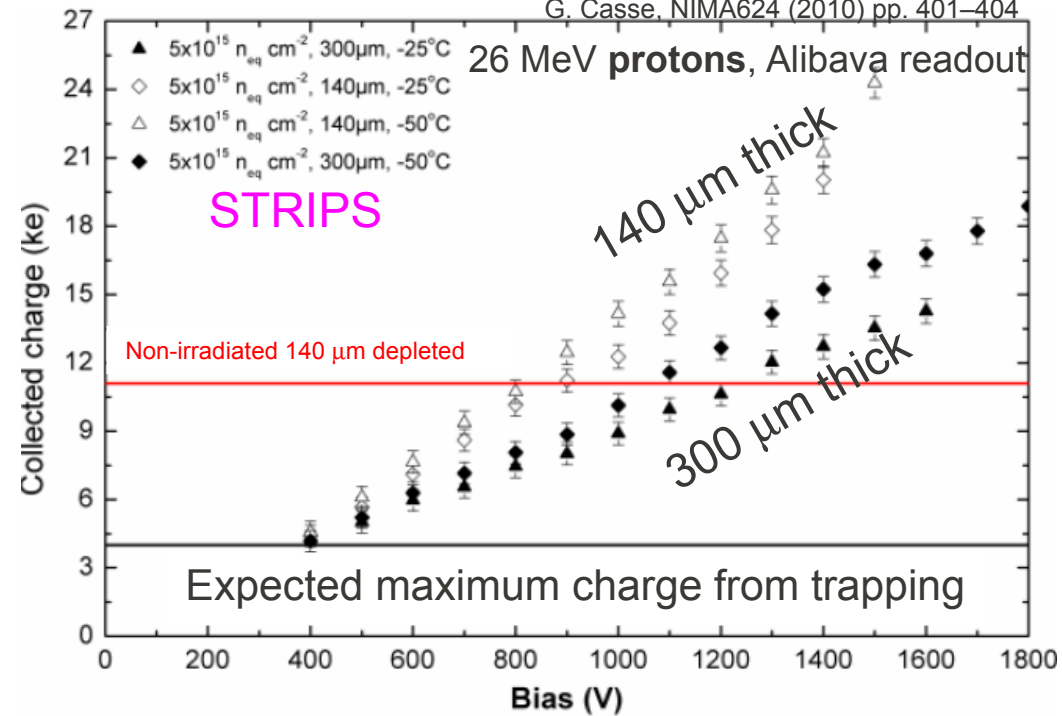
In general , the SNR will depend on the readout and individual sensor type

Charge Multiplication examples: strips, 3D

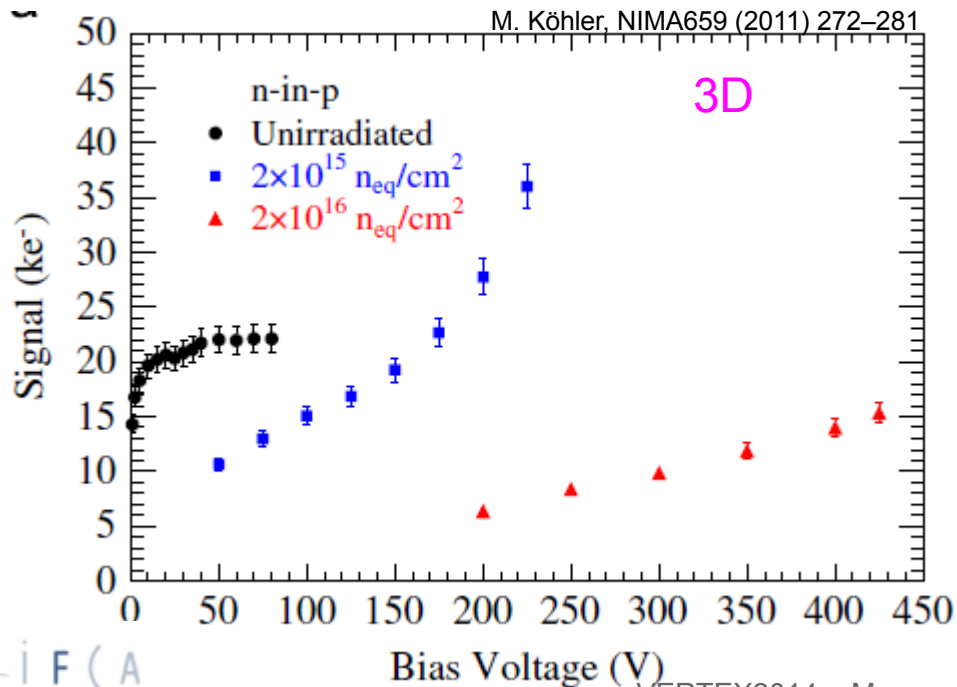
I. Mandic, NIMA 612(2010)474-477



G. Casse, NIMA624 (2010) pp. 401-404



M. Köhler, NIMA659 (2011) 272-281



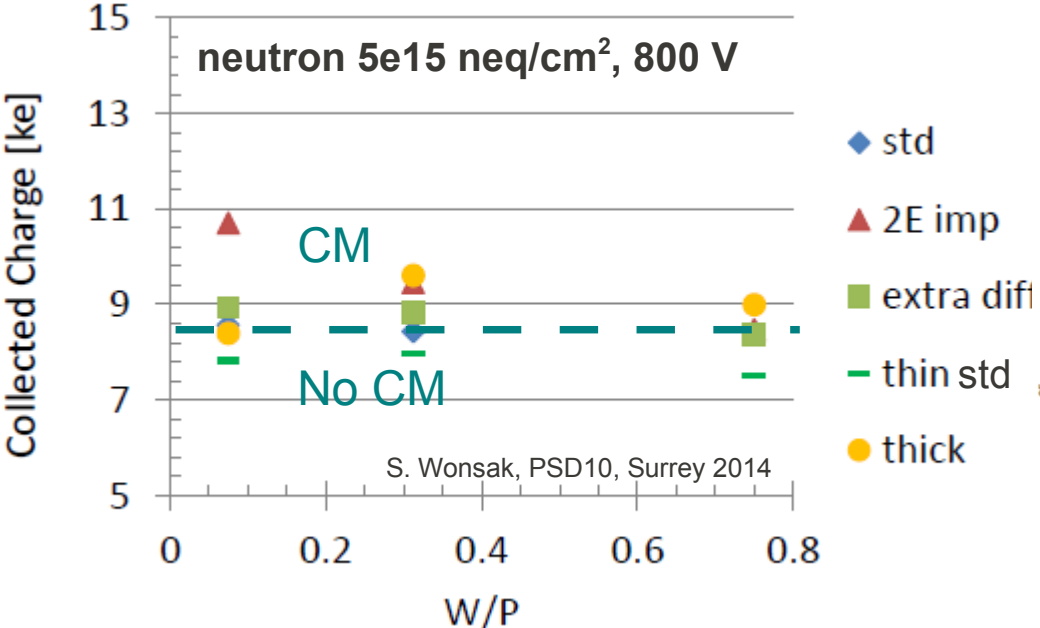
- Top left: The recovery of full charge collection only depends on the ability to provide a strong enough electric field to the sensor
- Top right: Charge collected by thin devices is higher than for thick ones (higher E-field for same voltage).
- Two **strategies** followed from here on:

- 1) **Junction engineering** to study and control amplification in irradiated devices
- 2) Detectors with **built in gain**

Charge multiplication via junction engineering

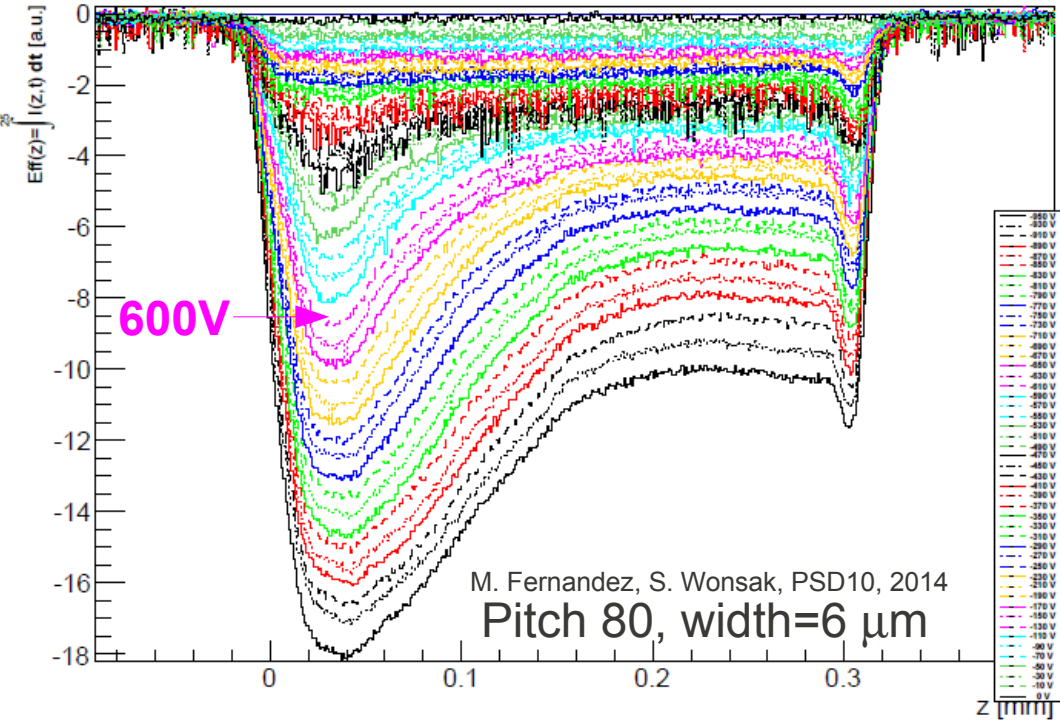
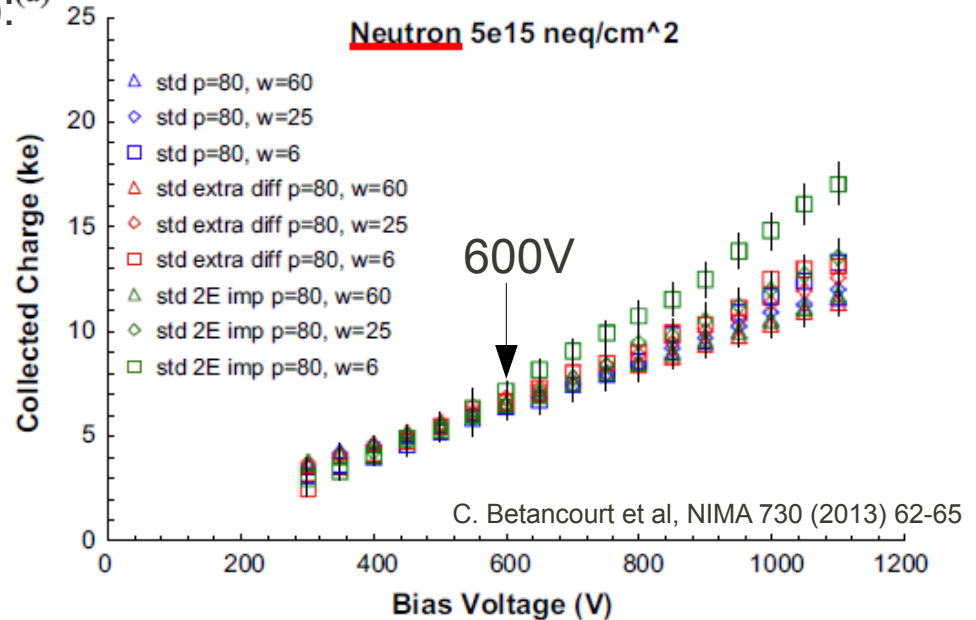
RD50 run of 5 wafers from Micron Sem. Ltd (UK):

- Varying w/p ratio, implant energy (2E imp), implant diffusion time (extra diff), with/without intermediate biased/floating strips, thickness (4×300 μm, 1×150 μm), resistivities (8-13 kΩ.cm)
- Irradiated with 23 MeV protons (1e15) or reactor neutrons (1e15, 5e15 n_{cm}²)



▪ Charge multiplication only observed at bias > 600V for neutron irradiated at 5e15 neq/cm²

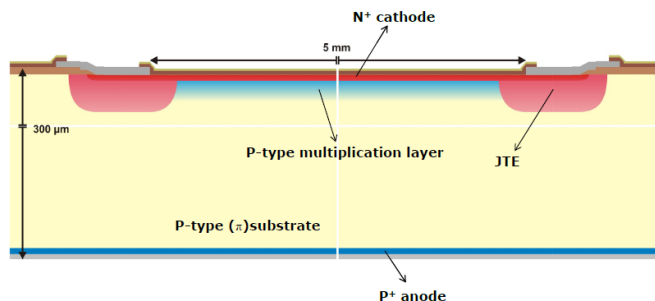
- Highest for “2E imp” and for lower w/p ratio (as expected since fields are larger at strip edges).
- Edge-TCT charge profiles clearly show gain region at the detector front. Multiplication appears when front junction dominates over backside junction.



Why low gain?

- Built in Low Gain allows read out using **same FE** as standard detectors.
- Thinner detectors can be produced to give the signal of thick ones. Noise can be kept moderated.

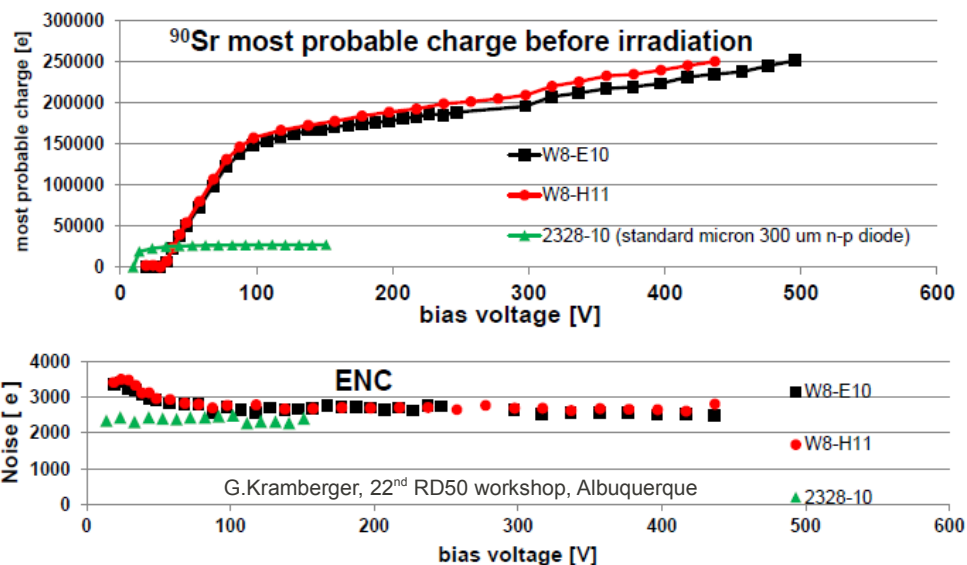
■ Technological challenge: control B implant dose to better than $2 \cdot 10^{12} \text{ cm}^{-2}$. Abrupt changes of gain for small changes of B implantation.



Technology:

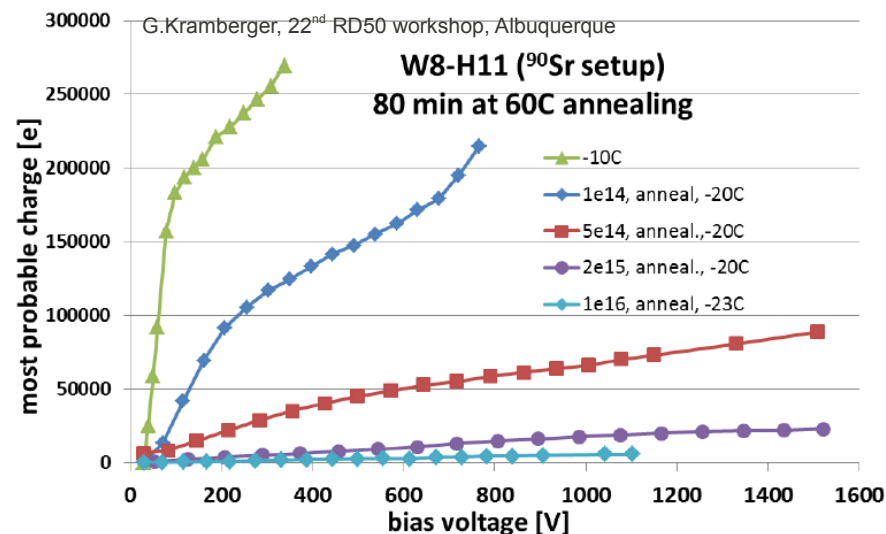
Based on APDs. An **extra p-type** layer (Boron) is diffused below the n+ electrode of a standard n-on-p detector. Under reverse bias, a high E-field is created in this region, and **impact ionization** leads to multiplication for electrons reaching n+ electrode.

Performance before irradiation



Gain $\sim \times 8$ at 300 V, no increase of noise

Performance after neutron irradiation



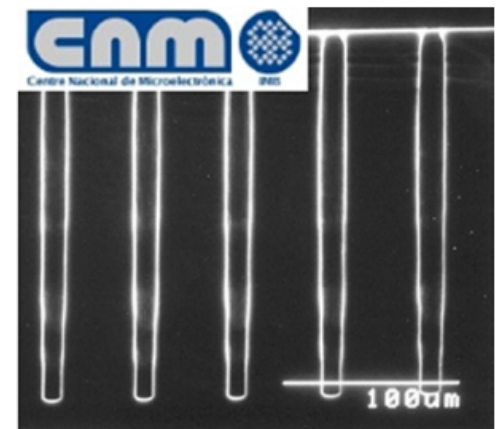
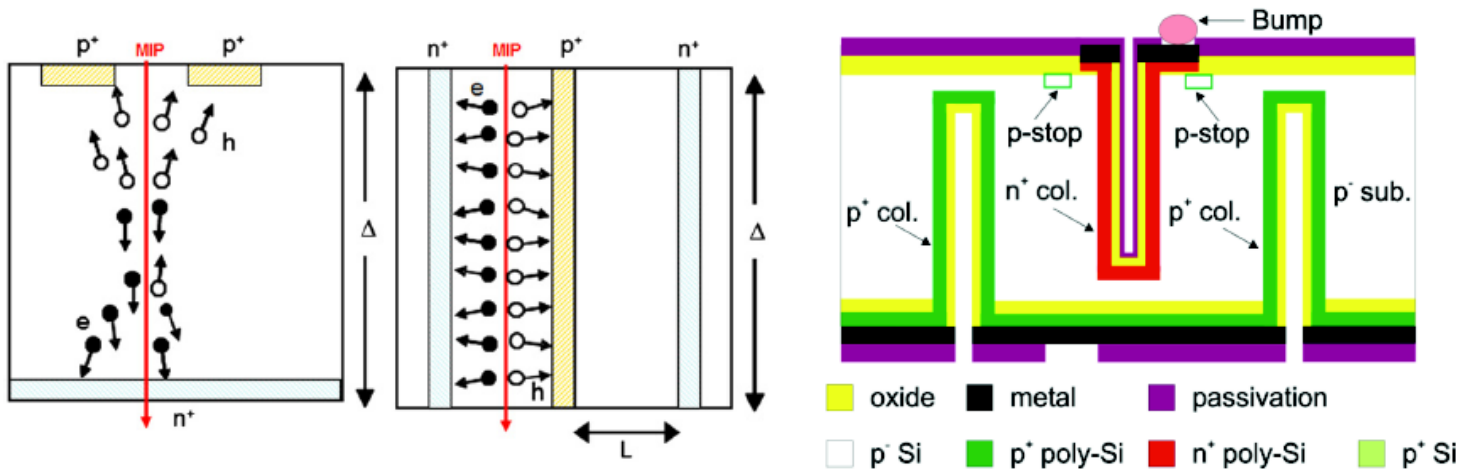
Effective acceptor removal in the p+ layer is responsible for gain degradation [G.Kramberger, 24th RD50, 2014]

- Investigation of other p-layer doping options: **different acceptor ions**

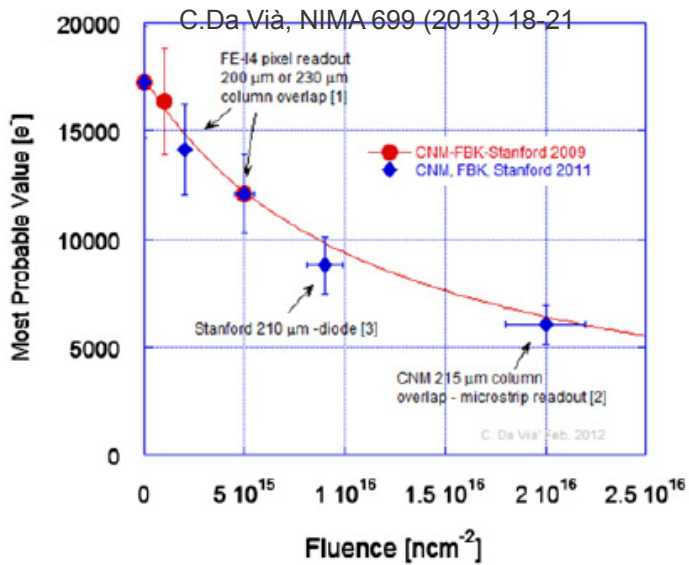
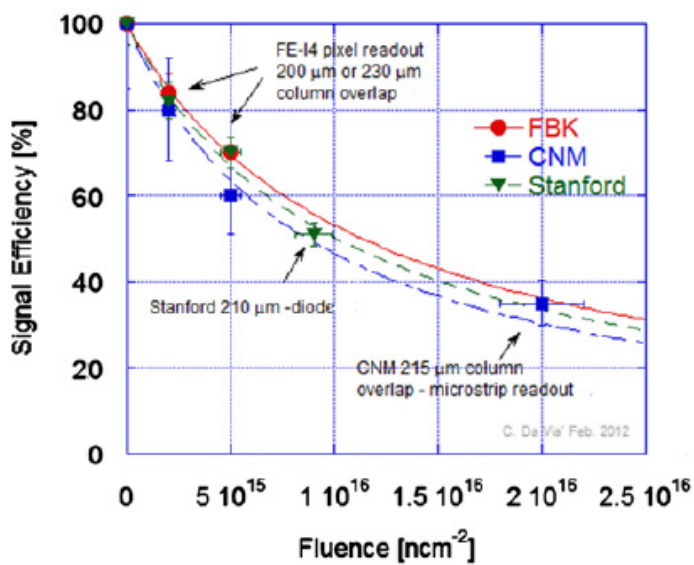
3D detectors

More info: S. Grinstein today

- In the road since 1997 (Parker et al.), they have been intensively studied by ATLAS community. Now populating 25% of ATLAS IBL. Commissioning taking place as of now.



- Maximum fluence at IBL is 5×10^{15} neq/cm² (conservative 3000 e threshold chosen)

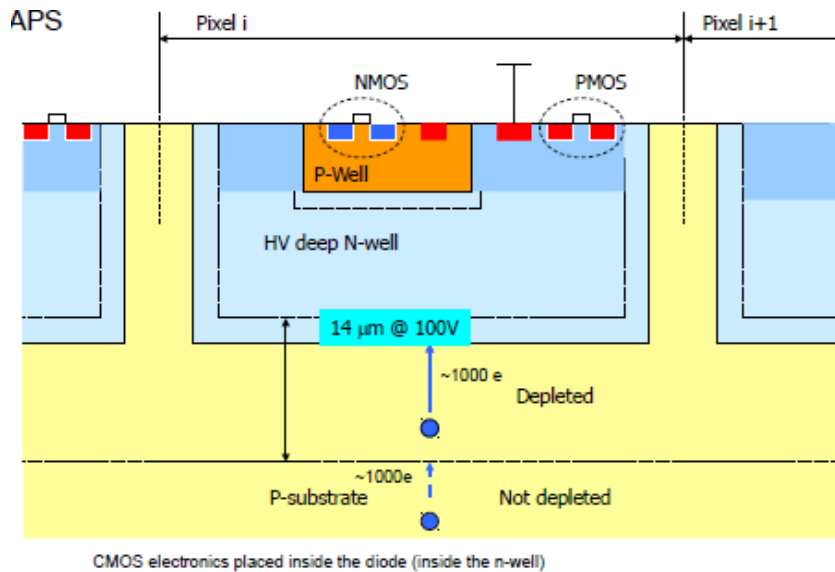


New RD50 project: exploring the capabilities of DRIE etching at cryogenic temperatures (40:1 aspect ratio)

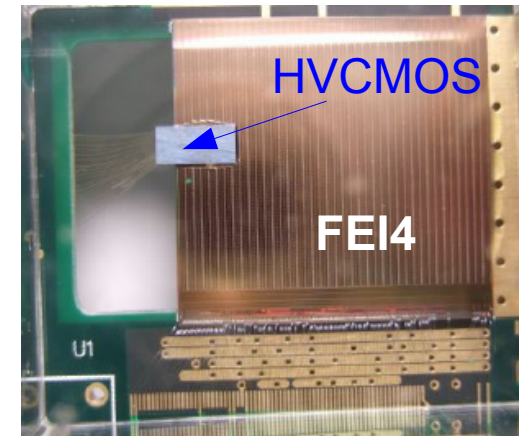
Near present:

New devices: HVCMOS

- Depleted active pixel detectors implemented in CMOS process. The sensor element is a deep n-well in a low resistivity ($\sim 10 \Omega \cdot \text{cm}$) p-type substrate. The main charge collection mechanism is drift in a very thin **depletion region** 10-20 μm . Substrate can be thinned down!



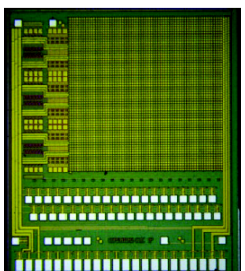
- Hit position encoded as height of the pulse in the pixel address line.
- AC coupling to the chip is possible. Successfully glued (not bump bonded) to ATLAS FE-I4 using flip-chip for alignment.



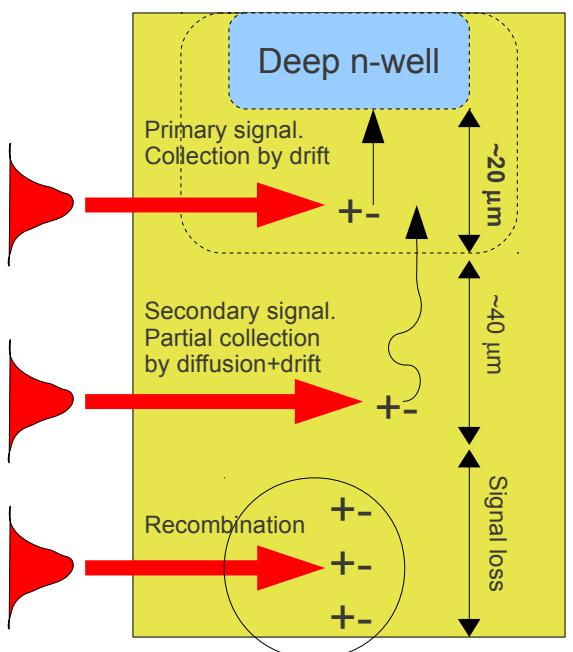
- Different readout geometries possible. For instance strip readout (summing pixels) using a standard RO chip (tests done with Alivaba).
- Proposed for the HL ATLAS upgrade, as pixel detector for Mu3e experiment (PSI) and Panda Luminosity Monitor.
- HVCMOS Collaboration includes: University of: Bonn, Geneva, Goettingen, Glasgow, Heidelberg; CERN, LBNL, CPPM.

HVCMOS: edge-TCT characterization

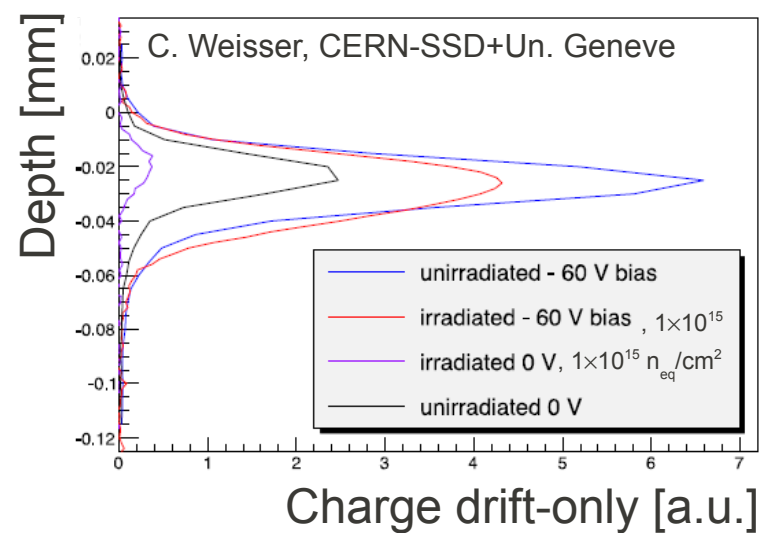
- HVCMOSv3 laser tested using edge-TCT technique (see G. Kramberger talk in this conference for edge-TCT details).



- Sampling induced current across the thickness of the detector using a collimated IR pulsed laser.

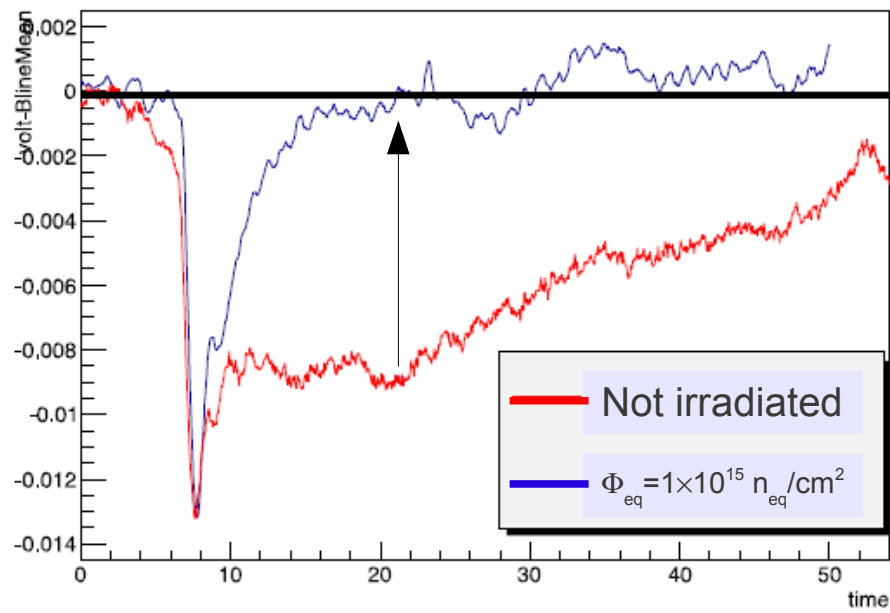
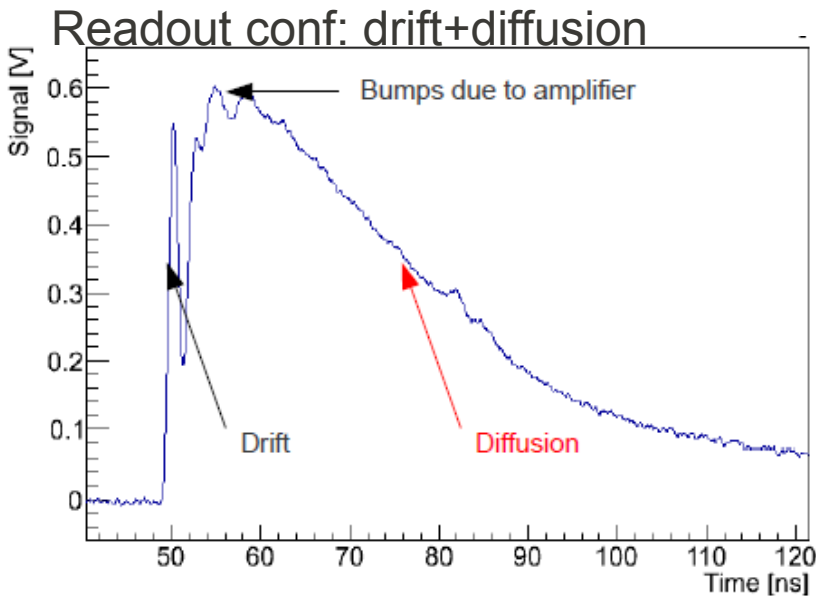


Side view of HVCMOS



- Scope readout: time resolved waveform

Very good performance for neutron irradiated detectors:



Room T measurement

Trapping kills slow diffusion component

Drift component remains almost invariant.

Summary

- RD50 is a CERN R&D collaboration. Common projects with experiments: Irradiation campaigns, test beams, wafer procurement and common sensor projects.
- RD50 is a transversal collaboration. Silicon experts from different experiments can come together and discuss/share information.
- Most of the activity focused on Si, in particular radiation hardness towards HL-LHC.
- Topics covered involve:
 - Defect characterization of Si (comprehensive map of defects)
 - Detector Characterization (including development of new characterization techniques like edge-TCT)
 - Device simulation (from excel spreadsheet to most complex TCAD machinery)
 - New structures (3Ds, thin detectors, slim edges, LGAD,...)
 - Full detector systems (Portable readout for Si microstrips: Alibava, comparison of producers, test beams...)

RD50 highlights

[from Michael Moll]

Some important contributions of RD50 towards the LHC upgrade detectors:

p-type silicon (brought forward by RD50 community) is now considered to be the base line option for the ATLAS and CMS Strip Tracker upgrade

n- MCZ (introduced by RD50 community) might improve performance in mixed fields due to compensation of neutron and proton damage: MCZ is under investigation in ATLAS, CMS and LHCb

Double column **3D detectors** developed within RD50 with CNM and FBK. Development was picked up by ATLAS and further developed for ATLAS IBL needs. They are an option for the CMS pixel upgrade.

RD50 results on very highly irradiated **planar segmented sensors** have shown that these devices are a feasible option for the **LHC upgrade**

RD50 data are essential input parameters for planning the running scenarios for LHC experiments and their upgrades (evolution of leakage current, CCE, power consumption, noise,....).

Charge multiplication effect observed for heavily irradiated sensors (diodes, 3D, pixels and strips). Dedicated R&D launched in RD50 to understand underlying multiplication mechanisms, simulate them and optimize the CCE performances. Evaluating possibility to produce fast segmented sensors?

Acknowledgements

Thanks to all members of RD50 collaboration for slides and plots included in this presentation

2009 Freiburg



Bari, June 2012



Albuquerque, June 2013



Bucharest, June 2014

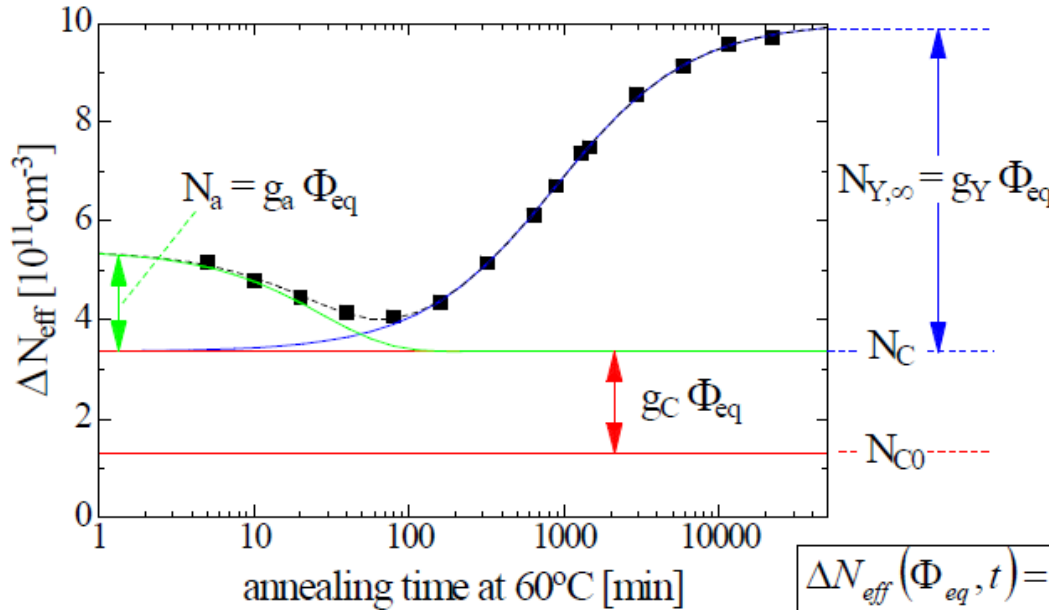


BACKUP

Hamburg model

$$\Delta N_{\text{eff}}(\Phi_{\text{eq}}, t) = N_{\text{eff}0} - N_{\text{eff}}(\Phi_{\text{eq}}, t)$$

ΔN_{eff} = Change of N_{eff} with respect to $N_{\text{eff}0}$ (value before irradiation)



long term reverse annealing:

$$N_Y = N_{Y,\infty} \cdot \left(1 - \frac{1}{1 + t/\tau_y} \right)$$

second order parameterization (with $N_{Y,\infty} = g_Y \times \Phi_{\text{eq}}$). gives best fit
But:

τ_y independent of Φ_{eq}
 \Rightarrow underlying defect reaction based on **first order process!**

$$\Delta N_{\text{eff}}(\Phi_{\text{eq}}, t) = N_a(\Phi_{\text{eq}}, t) + N_C(\Phi_{\text{eq}}) + N_Y(\Phi_{\text{eq}}, t)$$

short term annealing:

$$N_a = \Phi_{\text{eq}} \times \sum_i g_{ai} \times \exp\left(-t/\tau_i\right) = g_a \Phi_{\text{eq}} e^{-t/\tau_a}$$

first order decay of acceptors introduced proportional to Φ_{eq} during irradiation

stable damage:

$$N_C = N_{C0} \cdot (1 - \exp(-c \cdot \Phi_{\text{eq}})) + g_C \cdot \Phi_{\text{eq}}$$

incomplete „donor removal“
+ introduction of stable acceptors

M.Moll, Bethe Forum on Particle Detectors, Bonn – April 2014 -23-

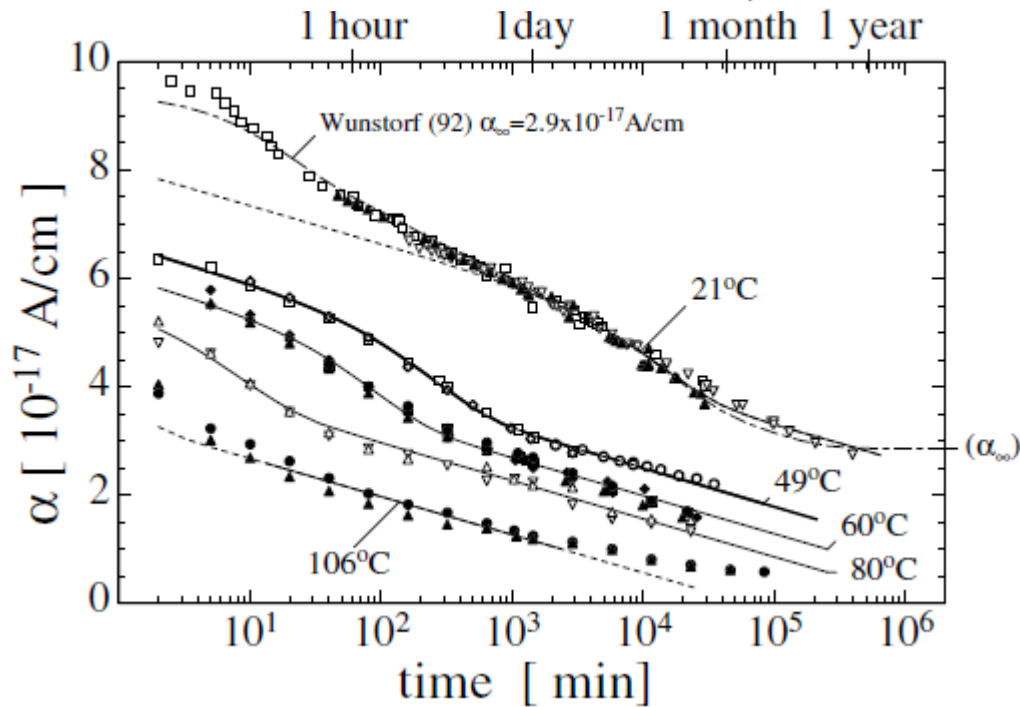
Beneficial ann.

T_a	-10°C	-7°C	0°C	10°C	20°C	40°C	60°C	80°C
τ_a	306 d	180 d	53 d	10 d	55 h	4 h	19 min	2 min
factor	1/134	1/78	1/23	1/5	1	16	174	1490

Reverse ann.

T_a	-10°C	0°C	10°C	20°C	40°C	60°C	80°C	100°C
τ_Y	516 y	61 y	8 y	475 d	17 d	1260 min	92 min	9 min
factor	1/396	1/47	1/6	1	29	544	7430	76650

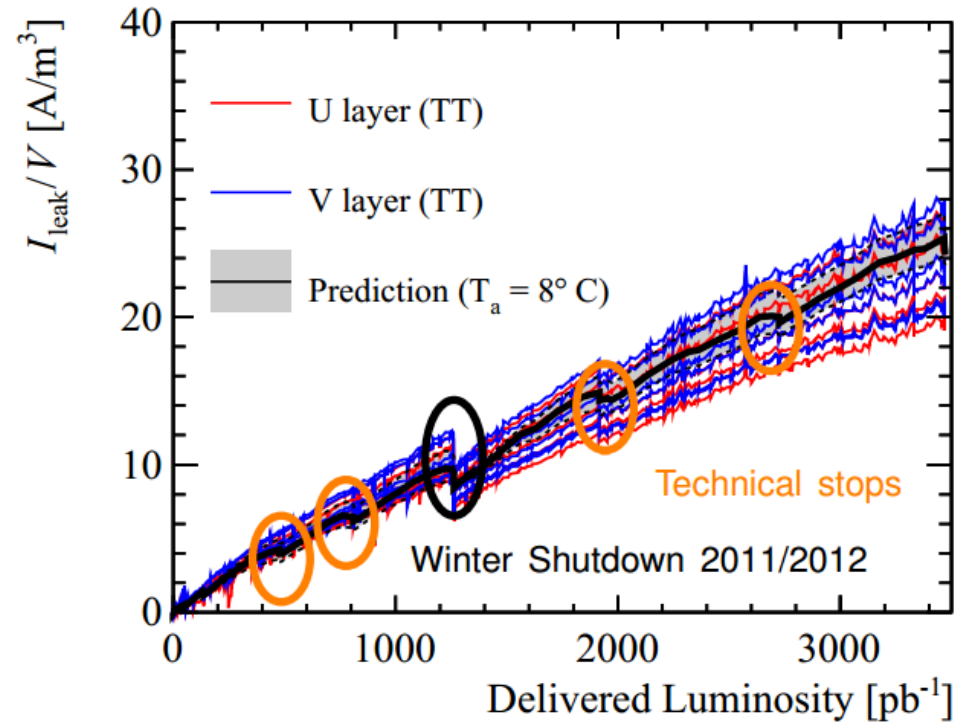
$$\frac{I_{\text{vol}}}{V} = \frac{I_{\text{vol}, \Phi=0}}{V} + \underbrace{\alpha \Phi}_{\Delta I_{\text{vol}}/V}$$



Leakage current decreases in time. If $\alpha \rightarrow 0$, then it would reach the same value as before irradiation
 Constant a is normally quoted after 80 min at 60C

The Temperature shown is the temperature at which the annealing is done. If the detector is left at room T, the leakage current after the technical stop will be smaller than if the detector was kept cold.

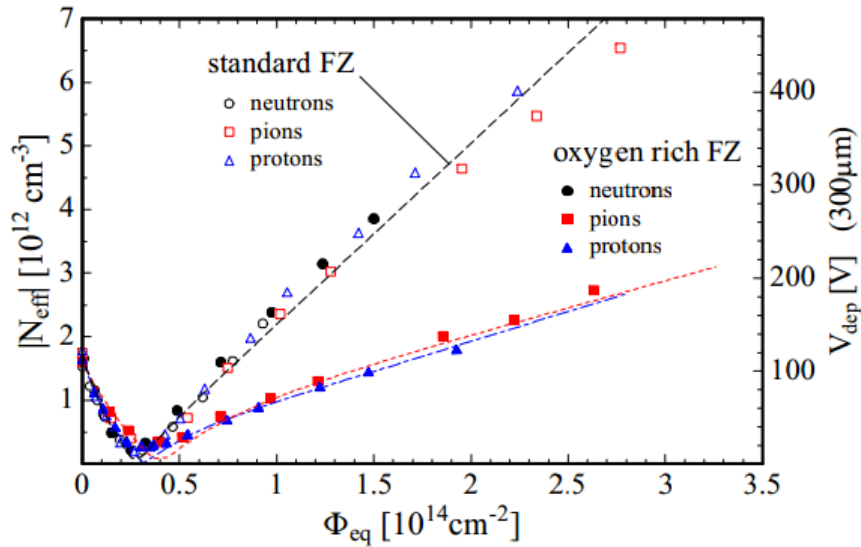
After 10 min at 106 C (for instance) $\alpha \sim 2.5 \times 10^{-17}$. If we start irradiating the detector at 20C, then the increase of leakage current is smaller than if we had annealed the sample at 21C



Vertex 2014 LHCb Silicon Detectors - Christian Elsasser

Dilemma:
 Leave detector cold and benefit from slower reverse annealing
 or warm the detector and benefit from I_{leak} annealing

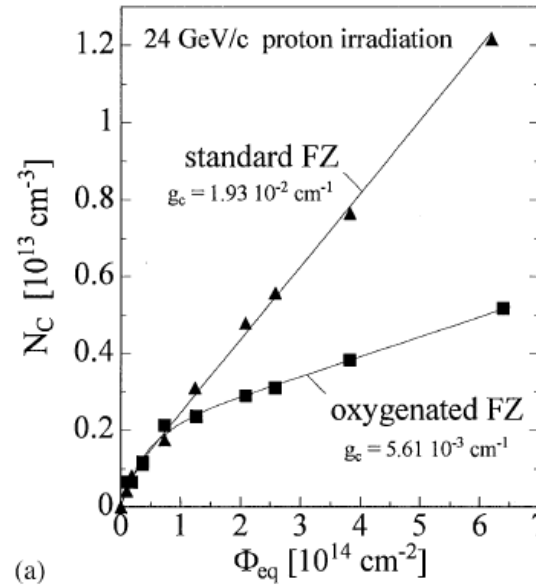
Virtues of DOFZ



G. Lindstroem, CERN-RD48, LEB-workshop, Cracow 14-Sep-00

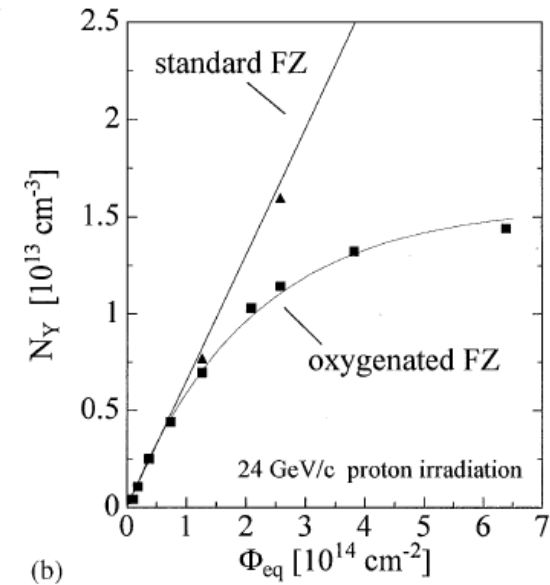
Strong reduction (w.r.t. “standard silicon”) of V_{dep} after 24 GeV/c proton and 300 MeV/c pion irradiation

Unchanged after reactor neutrons



G. Lindström, Volume 466, Issue 2, 1 July 2001, Pages 308–326

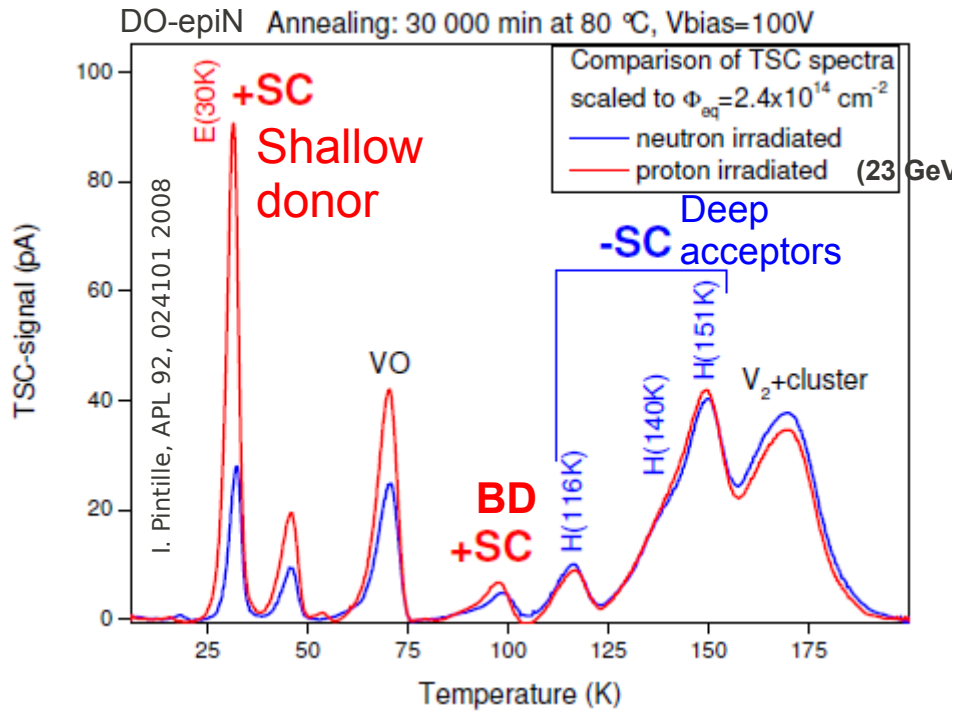
Stable damage (acceptor introduction) improved by a factor 3.



Saturation of reverse annealing

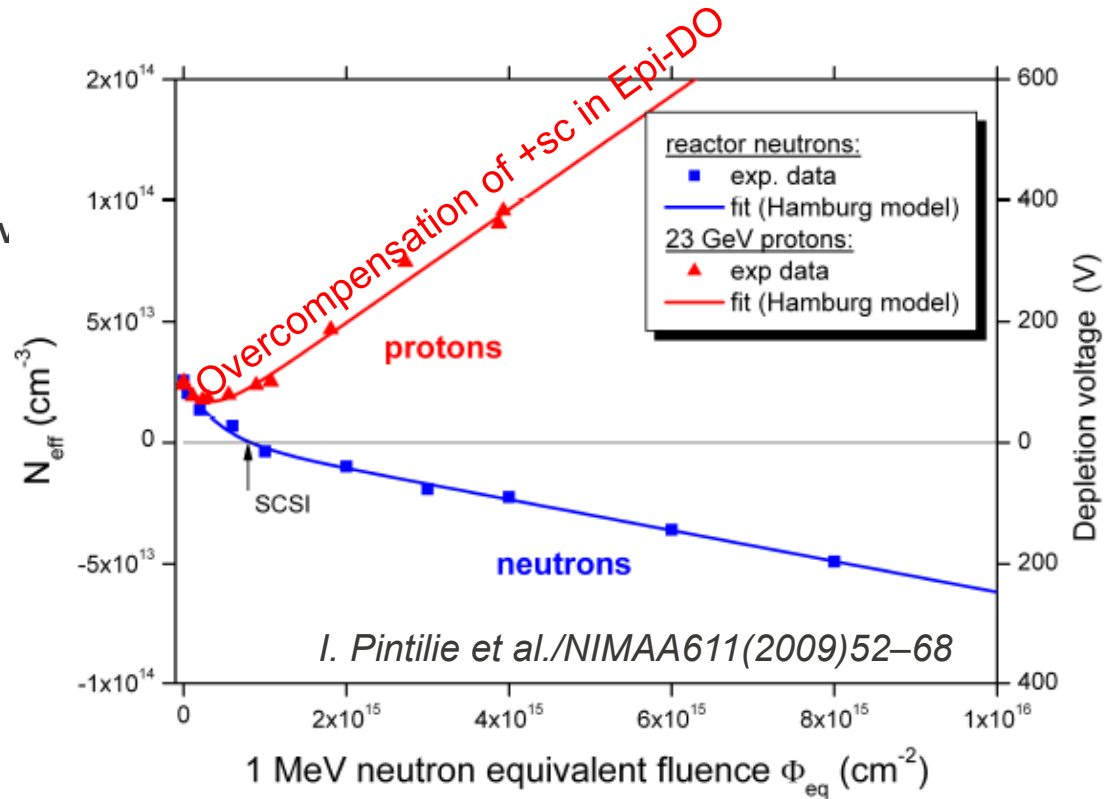
Defects with impact on Neff

- Significant progress over last few years identifying defects responsible for sensor degradation after neutron and proton irradiation. Defects related to N_{eff} (left) and N_{eff} reverse annealing (right)



– Identified **shallow donors** [E(30K) and BD] in O-rich epi-Si with higher concentration after proton than after neutron irradiation. They contribute with +sc. VP process also suppressed

The concentration of +sc overcomes that of **deep acceptor** (-sc). As a consequence no type inversion after proton irradiation seen in O-rich materials.

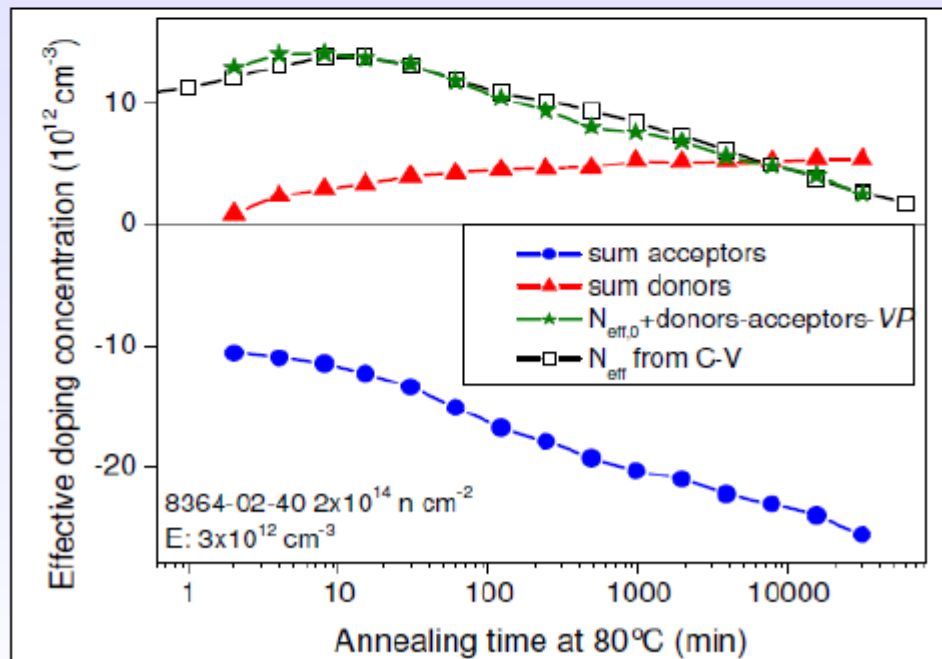


The peaks for deep acceptors (identified as hole traps, H(116K), H(140K), H(152K)) responsible for reverse annealing. Observed concentration increase with time at 80 C.

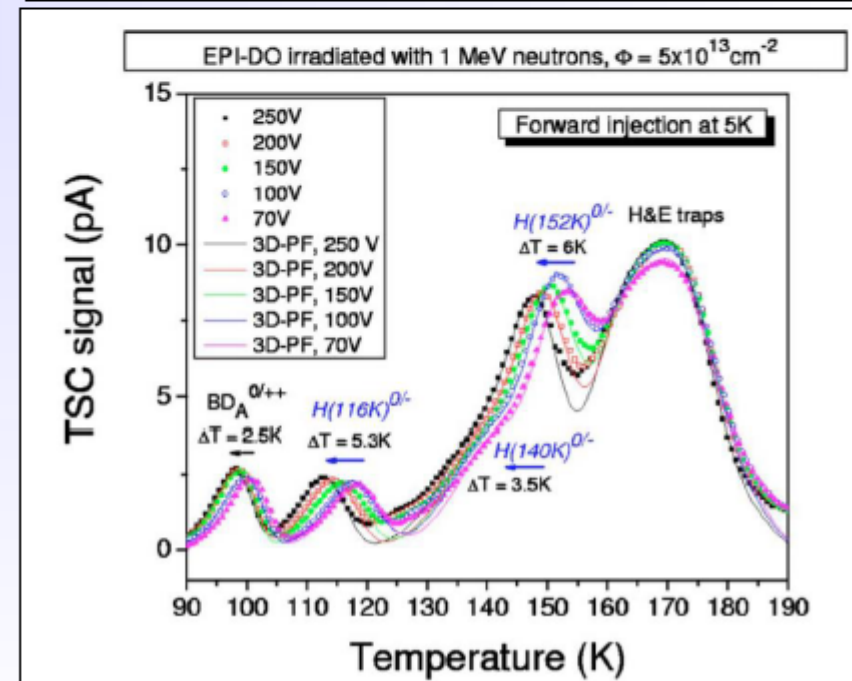
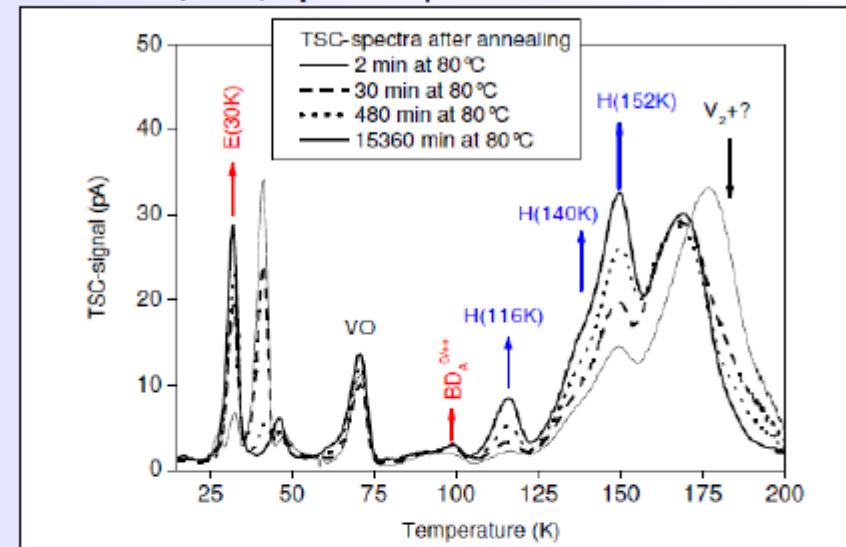
Top right: For short annealing times around the minimum of N_{eff} the large E(30K) concentration after proton irradiation leads to an over-compensation of the deep hole centers and thus, in contrast to neutron damage, the effective doping remains positive, increasing with fluence.

Defects

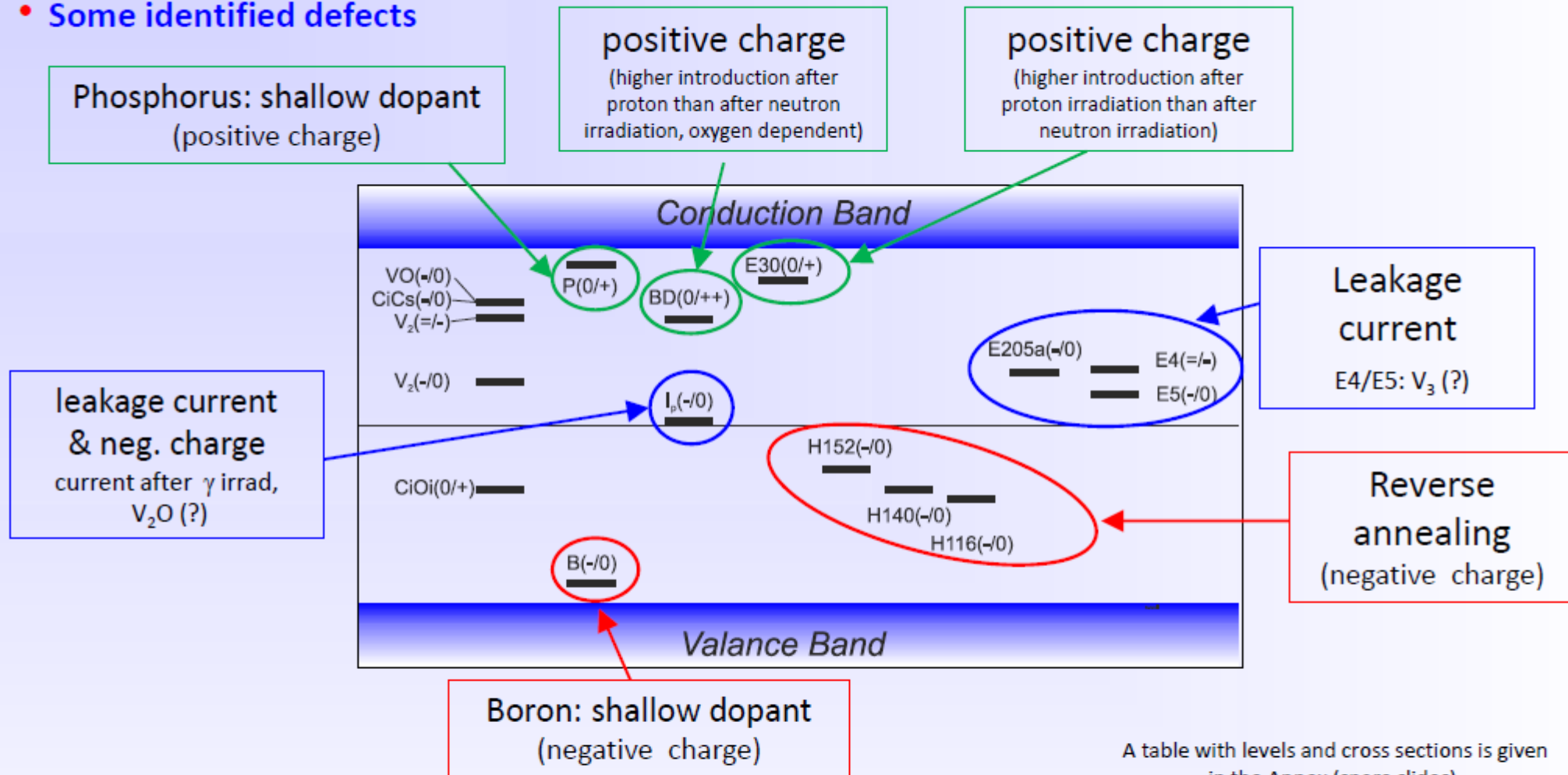
- **Macroscopic observation:**
 - Irradiated silicon sensor show “reverse annealing” (negative space charge increasing with time)
- **Example: Neutron irradiated epitaxial silicon**
 - Identification of hole traps that grow with reverse annealing and are deep acceptors (labelled: $H(116K)$, $H(140K)$, $H(152K)$)
 - Absolute correlation of defect concentration to increase of $|N_{\text{eff}}|$ (reverse annealing)



$2 \times 10^{14} \text{ n/cm}^2$, Epi-St $75 \mu\text{m}$



- Some identified defects



- **Trapping: Indications that E205a and H152K are important** (further work needed)
- Converging on consistent set of defects observed after p , π , n , γ and e irradiation.
- Defect introduction rates are depending on particle type and particle energy and (for some) on material!

- Some defects observed after electron irradiation (1.5 to 15 MeV)

Results consistent with previous RD50 works on hadron damage

Defects	σ_n [cm ²]	σ_p [cm ²]	E_A [eV]	Assignment/References	Impact on the diodes electrical characteristics at room temperature
E(30K)	2.3×10^{-14}		$E_C - 0.1$	Electron trap with a donor level in the upper half of the Si bandgap / [11]	On the N_{eff} by introducing positive space charge
H(40K)		1.7×10^{-15}	$E_V + 0.09$	Hole trap/[11]	
VO_1^{-0}	1.44×10^{-14}		$E_C - 0.176$	VO_1^{-0} / [40]	
$C_1C_2^{-0}$	1.4×10^{-14}		$E_C - 0.171$	$C_1C_2^{-0}$ / [41, 42]	
I_p^{+0}	1.7×10^{-15}		$E_V + 0.23$	Donor level of V_2O or of a still unknown C related defect/[11, 30]	
$I_p^{0/-}$	1.7×10^{-15}	9×10^{-14}	$E_C - 0.55$	Acceptor level of V_2O or of a still unknown C related defect/[11, 30]	On the N_{eff} by introducing negative space charge and on LC
C_1^{+0}	1.11×10^{-15}	4.28×10^{-15}	$E_V + 0.284$	C_1^{+0} / [21]	
V_2^{-0}	2.1×10^{-15}		$E_C - 0.424$	V_2^{-0} / [21]	
E_4	1×10^{-15}		$E_C - 0.38$	$V_3^{-/}$ / [38]	On LC
E_5	7.8×10^{-15}		$E_C - 0.46$	V_3^{-0} / [38]	On LC
H(116K)		4×10^{-14}	$E_V + 0.33$	Hole trap with an acceptor level in the lower part of the Si bandgap - Extended defect (cluster of vacancies and/or interstitials) / [10,11]	On the N_{eff} by introducing negative space charge
H(140K)		2.5×10^{-15}	$E_V + 0.36$	Hole trap with an acceptor level in the lower part of the Si bandgap - Extended defects (clusters of vacancies and/or interstitials)/[10,11]	On the N_{eff} by introducing negative space charge
H(152K)		2.3×10^{-14}	$E_V + 0.42$	Hole trap with an acceptor level in the lower part of the Si bandgap - Extended defects (clusters of vacancies and/or interstitials)/[10,11]	On the N_{eff} by introducing negative space charge
H(87K)		0.3×10^{-15}	$E_V + 0.193$	V_3^{0+} / [37]	
H(98K)		1.2×10^{-15}	$E_V + 0.234$	$V_2O^{0+} + V_3O^{0+}$ / [37]	

- BD defect:

- $E_i^{BD} = E_C - 0.225 \text{ eV}$
- $\sigma_n^{BD} = 2.3 \cdot 10^{-14} \text{ cm}^2$

- Converging on consistent set of defects observed after proton, pion, neutron, gamma and electron irradiations by various techniques (Introduction rates depend of course strongly on the type of irradiation and for some of the defects on the material.)

Choice of Material for HL-LHC

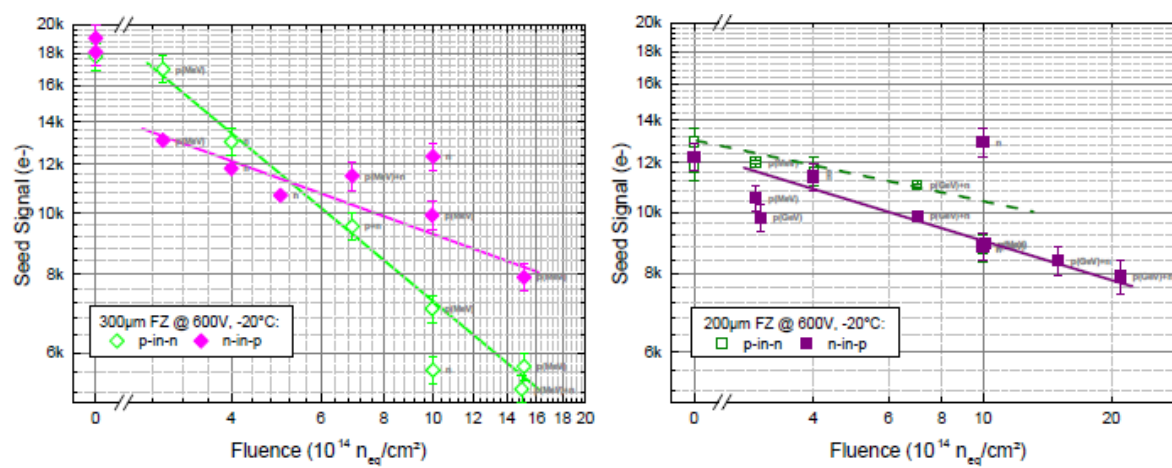


Figure 11: Charge collected on the seed strip (strip with the highest signal in a cluster) vs. fluence for 600 V biasing at -20°C after short annealing (50 h to 250 h) at room temperature, for sensor thickness of $320\ \mu\text{m}$ (left) and $200\ \mu\text{m}$ (right). Lines are drawn to guide the eye.

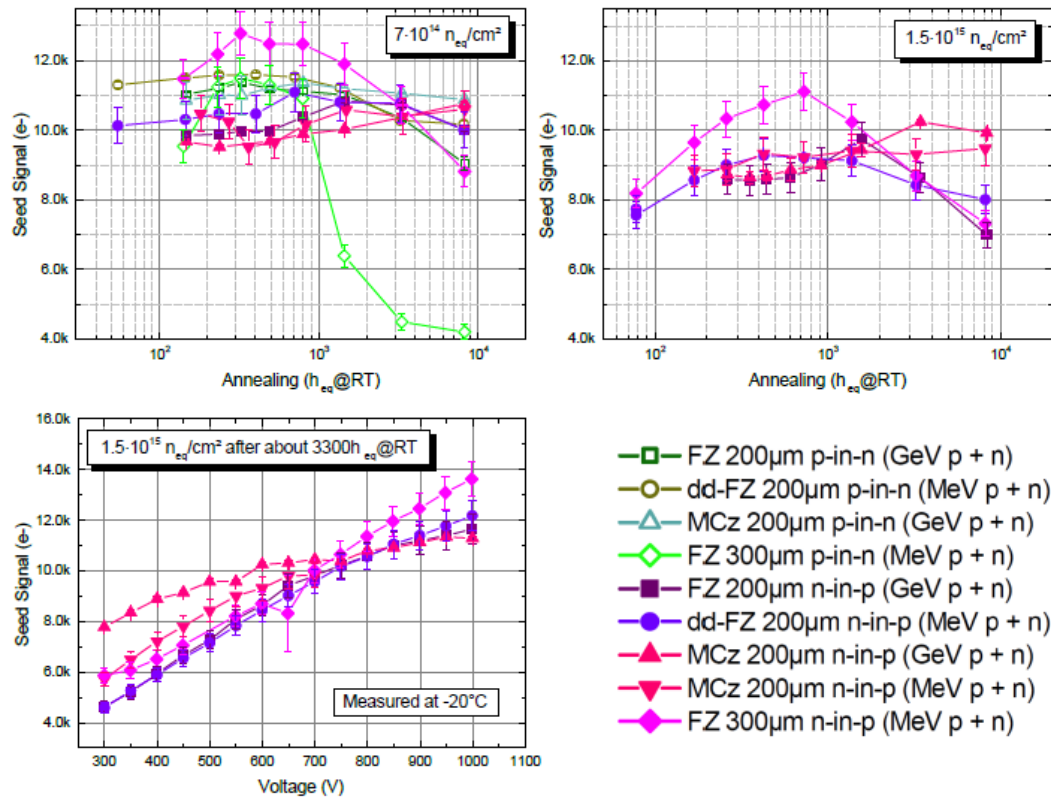


Figure 12: Top: charge collection at 600 V and -20°C vs. equivalent annealing time at room temperature (RT), for two different irradiation levels. Bottom: charge collection vs. bias voltage after $1.5 \cdot 10^{15}\ \text{n}_{\text{eq}}\ \text{cm}^{-2}$ and 3300 h equivalent annealing at room temperature.

- Optimizing the sensor thickness
- Measurement of thin FZ p-type pixel sensors: 75, 100, 150 and 285 μm (MPI/CIS)

From M.Moll VERTEX 2013 proceedings

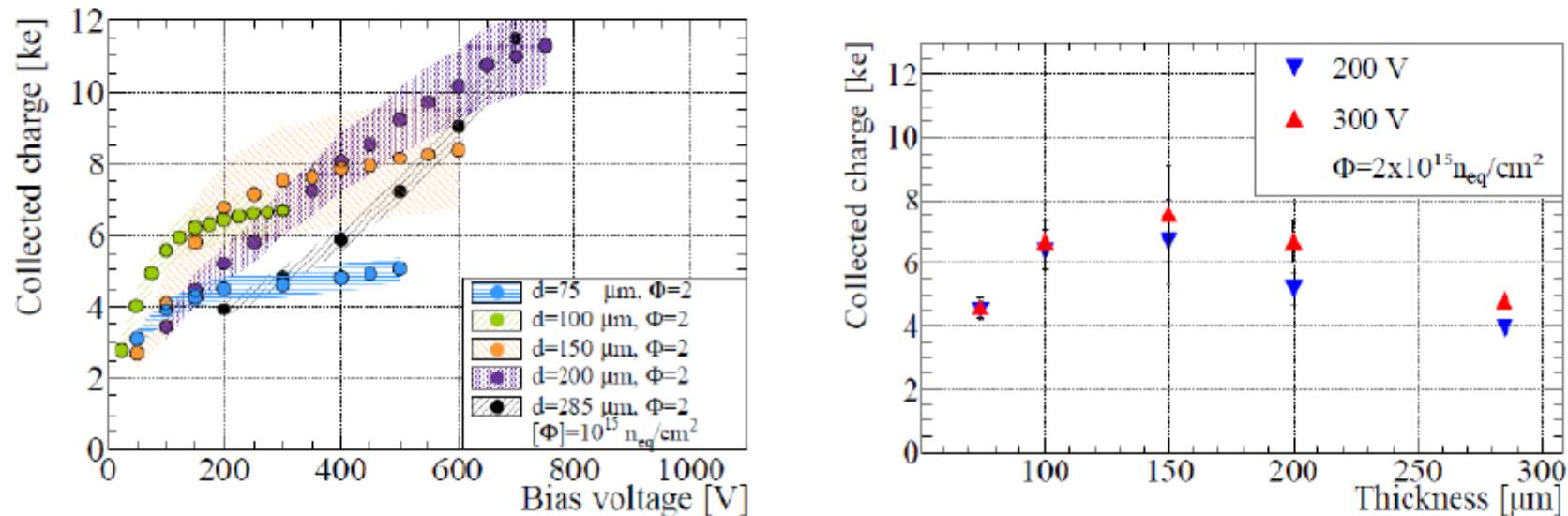


Figure 4: Comparison of collected charge as measured with a Sr^{90} source on irradiated ($\phi_{eq} = 2 \times 10^{15} \text{ n}_{eq} \text{ cm}^{-2}$) p-type pixel sensors with different thickness bump-bonded to ATLAS FEI4 readout chips [23]. Left: Collected charge as function of voltage. Right: Collected charge as function of device thickness for 200V and 300V.

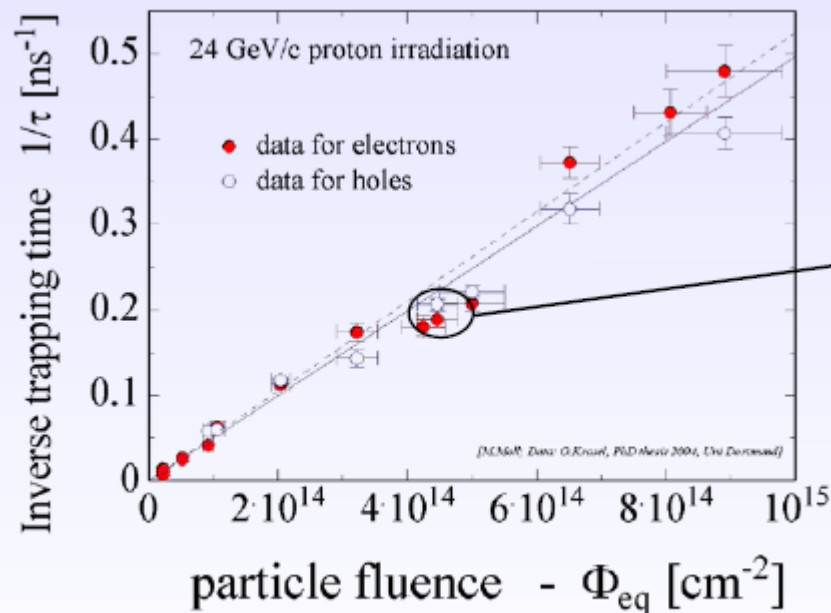
[23] S.Terzo. Irradiated n-in-p planar pixel sensors with different thicknesses and active edge designs. *23rd RD50 Workshop, November 2013.*

■ Deterioration of Charge Collection Efficiency (CCE) by trapping

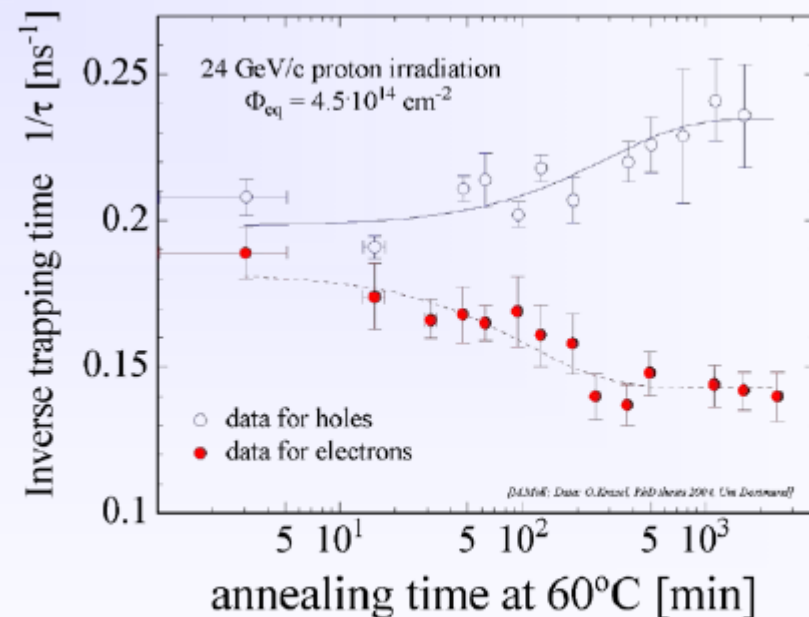
Trapping is characterized by an effective trapping time τ_{eff} for electrons and holes:

$$Q_{e,h}(t) = Q_{0,e,h} \exp\left(-\frac{1}{\tau_{\text{eff } e,h}} \cdot t\right) \quad \text{where} \quad \frac{1}{\tau_{\text{eff } e,h}} \propto N_{\text{defects}}$$

Increase of inverse trapping time ($1/\tau$) with fluence



..... and change with time (annealing):

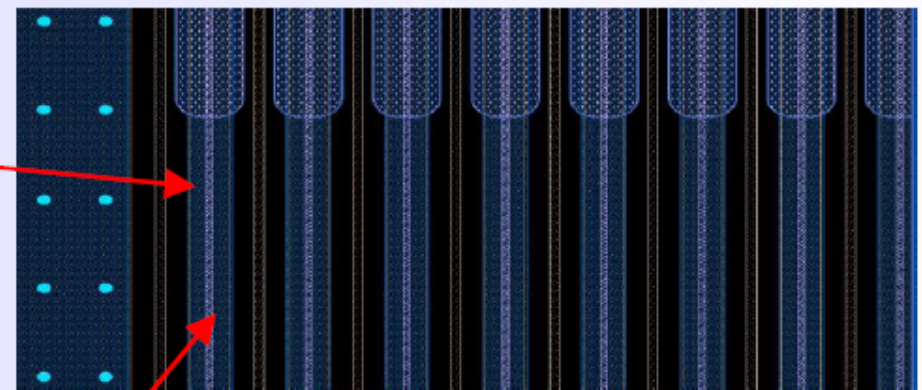
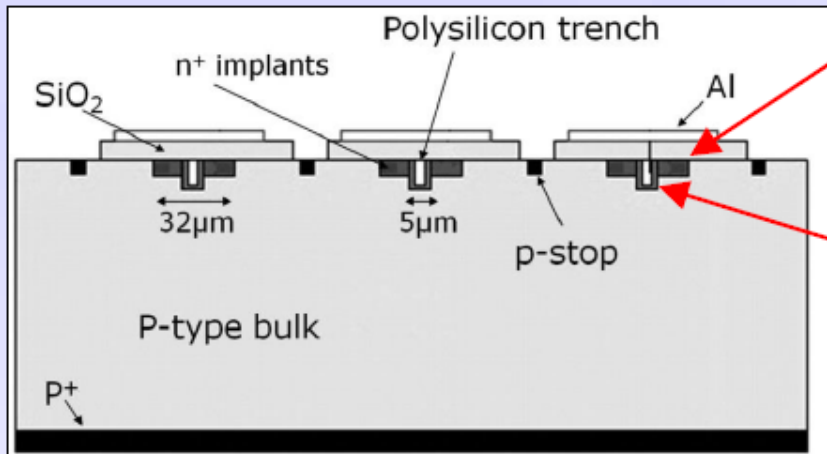


New structures

[G.Casse et al., NIMA 669 (2013) 9-13]

Strip detector design with trenches

- 5, 10, 50 μm deep trenches
- 5 μm wide in center of n^+ electrode

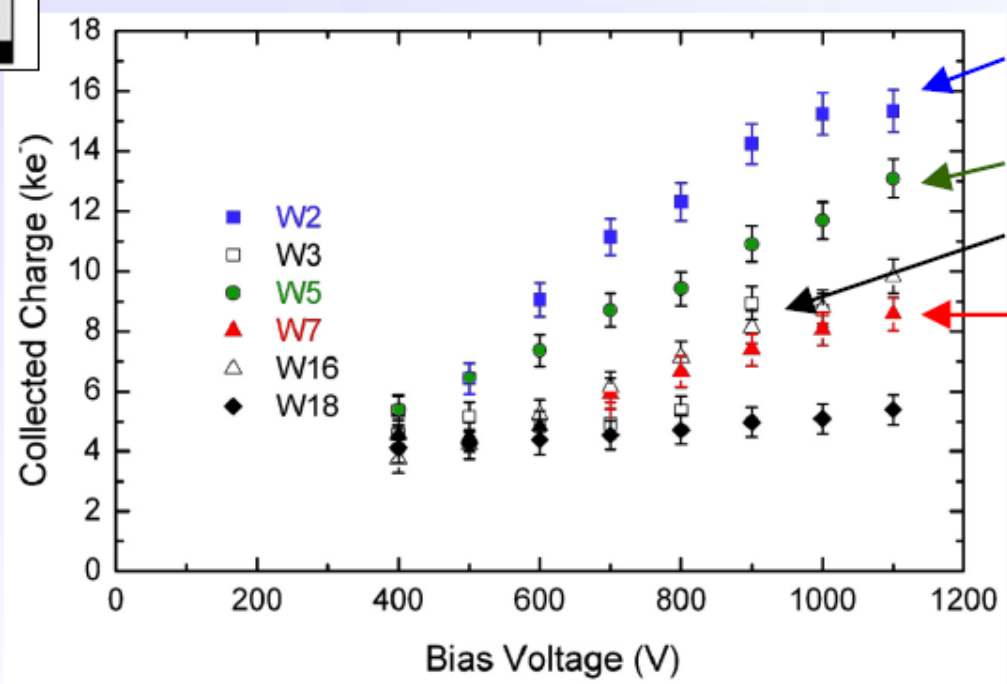


Implant

Poly trench n-doped

Sizeable effect on Charge Multiplication

- Irradiation: $5 \times 10^{15} \text{ n}_{\text{eq}} \text{ cm}^{-2}$ (neutrons)
- Significant difference in CCE between standard and trenched detectors (-25°C)
- However, not evident how gain relates to depth of trench



trench depth

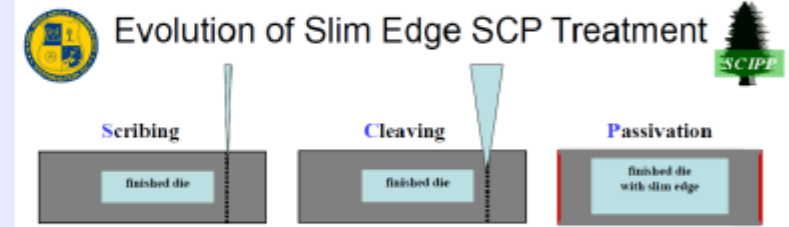
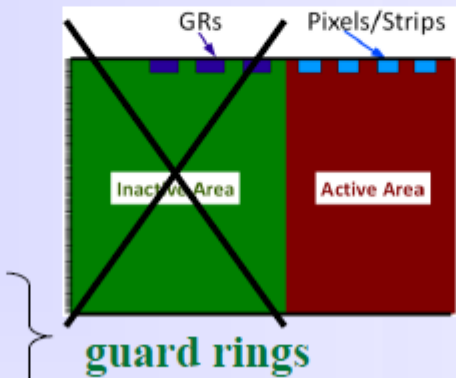
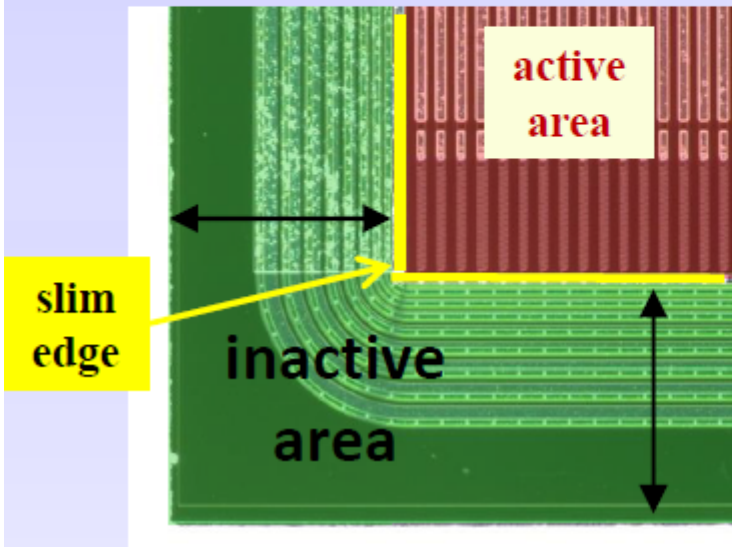
5 μm trench

50 μm trench

10 μm trench

standard

- RD50 slim edges project (reduce dead space around the active sensor)



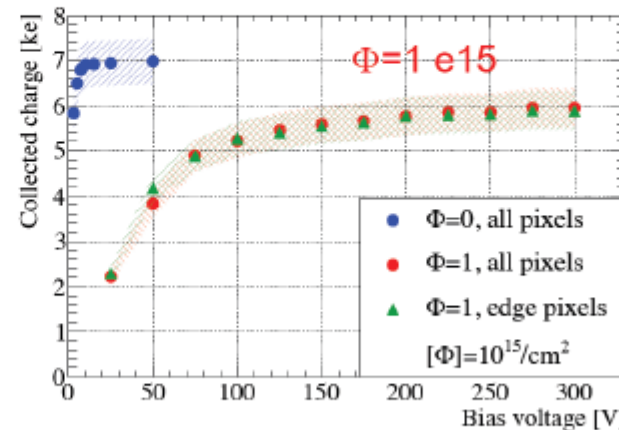
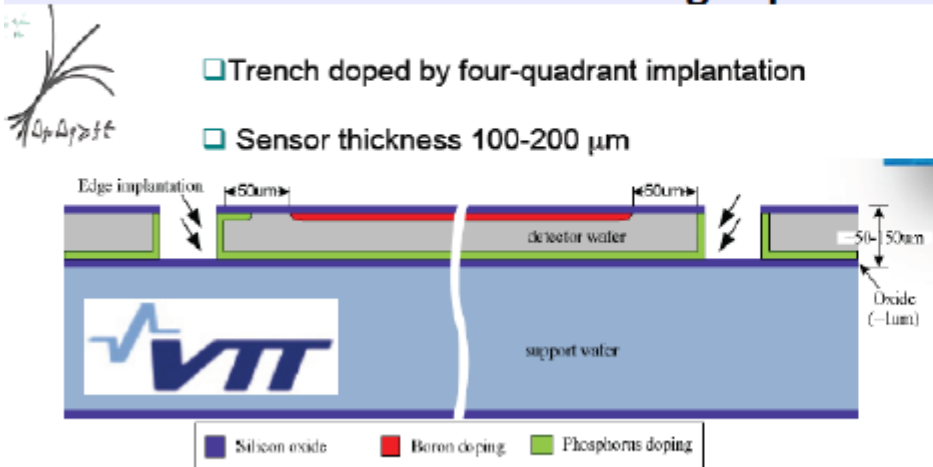
- Scribe** XeF₂ etch, diamond scribe, DRIE
- Cleave** automated, manual
- Passivate** nitride, oxide (n-type)
alumina ALD (p-type)

[V. Fadeyev, 22nd RD50 Workshop, Albuquerque, June 2013]

... development picked up by HPK (see Hiroshima Symposium 9/2013)

- Active edges (VTT & MPI Munich)

- Thin wafers with active edges produced at VTT [A. Macchiolo, 22nd RD50, Albuquerque, June 2013]



10^{15} p/cm^2

Testbeam:
no difference between edge and other pixel!

- FE-I3 100 µm thick sensor with 125 µm slim edge, threshold 1500 e⁻ → 87% CCE at 300 V for both all and edge pixels after irradiation at KIT